

MADRIGAL, KARLA E, M.S. Refinement of the Conformation of Selected Transmembrane Helices in the Cannabinoid Receptor GPR55 using Conformational Memories (CM). (2011)

Directed by Dr. Patricia H. Reggio, 76 pp.

GPR55 is a newly de-orphanized cannabinoid receptor which belongs to the class A G-protein coupled receptors (GPCRs) family and binds constituents of the plant, *Cannabis sativa*. It has been suggested that the manipulation of GPR55 may have a therapeutic potential in the treatment of inflammatory and neuropathic pain.

The purpose of the present study was to refine the transmembrane helices (TMH) conformation in GPR55 that have significant sequence divergence from other class A GPCRs. The methods used were conformational memories (CM) to refine the transmembrane helices (TMH) of TMH2, TMH5, TMH6 and TMH7. The results of these calculations were used to modify the GPR55 computer model initially built in Reggio lab based on a rhodopsin template to generate refined inactive and active models of GPR55.

The average proline kink angle and standard deviation for each set of conformational results generated by CM were measured using the Prokink program. A statistical analysis of the resultant face shift, wobble angle and bend angle of the helices containing proline was performed using the one sample t test and compared to the  $\beta$ -2 adrenergic receptor.

The refined model of the inactive receptor of GPR55 obtained from the conformational memories is shown in figure 1. In conclusion the results of conformational memories are consistent with the proposal of Ballesteros, that even though the overall structure of rhodopsin and other class A GPCRs may be very similar, there are localized regions where the structures of these receptors diverge. A significant range of conformational diversity could be generated by the presence of Pro-kinks and Cys/Ser/Thr residues. The results obtained should help to define the mechanism of

drug receptor interaction relevant to cannabinoid physiological and pathophysiological functions including drug abuse.

REFINEMENT OF THE CONFORMATION OF SELECTED TRANSMEMBRANE  
HELICES IN THE CANNABINOID RECEPTOR GPR55 USING  
CONFORMATIONAL MEMORIES (CM)

by

Karla E. Madrigal

A Thesis Submitted to  
The Faculty of The Graduate School at  
The University of North Carolina at Greensboro  
in Partial Fulfillment  
of the Requirements for the Degree  
Master of Science

Greensboro  
2011

Approved by

---

Committee Chair

To my father who was always my inspiration.

You could not be here next us but

You will be always in our heart.

## APPROVAL PAGE

The thesis has been approved by the following committee of the Faculty of The Graduate School at The University of North Carolina at Greensboro.

Committee Chair \_\_\_\_\_

Committee Members \_\_\_\_\_

\_\_\_\_\_

\_\_\_\_\_

\_\_\_\_\_  
Date of Acceptance by Committee

\_\_\_\_\_  
Date of Final Oral Examination

## ACKNOWLEDGEMENTS

I would like to acknowledge the advice and guidance of my advisor Dr. Patricia Reggio and also her lab staff, especially the research scientist Dow Hurst for his knowledge and assistance during my thesis research.

I acknowledge the NIDA RO1 DA023204 for their financial support for this project and I would like to thank Banner Pharmacaps, Inc. for all his support, especially Dr. Aqeel Fatmi.

I also thank the members of my graduate committee, Dr. Banks and Dr. Duffy for their guidance and suggestions. And I would like to thank my family members, especially my husband Chidu for supporting and encouraging and my son Namin for letting me to pursue this degree.

## TABLE OF CONTENTS

	Page
LIST OF TABLES .....	vii
LIST OF FIGURES .....	viii
 CHAPTER	
I. INTRODUCTION .....	1
GPR55 .....	2
GPCR Structure and Function .....	10
II. OBJECTIVE .....	17
III. METHODS .....	18
Molecular Modeling .....	18
Side chain conformation.....	19
Models of TMH 2, TMH 5, TMH 6 and TMH 7 for GPR55 .....	21
Conformational Memories (CM).....	23
Exploratory phase.....	24
Biased annealing phase .....	25
Metropolis criterion .....	25
Variable bond angles .....	26
Evaluation of CM Output .....	26
Helix Choice for TMH Bundle.....	27
Presence of proline in $\alpha$ Helices .....	28
Bend angle and wobble angle definition .....	30
Sequence Dictated Divergence.....	32
R and R* Model Refinement.....	33
IV. RESULTS .....	34
TMH2 .....	34
TMH5 .....	38
TMH6.....	41
TMH7 .....	45
Helix 8 GPR55 .....	48

Model of Inactive state (R) and active state form of GPR55 .....	48
V. DISCUSSION .....	50
TMH2 .....	50
TMH5 .....	51
TMH6 .....	52
TMH7 .....	57
VI. CONCLUSIONS .....	59
REFERENCES .....	60



## LIST OF TABLES

	Page
Table 1. Comparative table of the different GPR55 ligands.....	7
Table 2. Summary of GPCR Activation .....	13
Table 3. Comparison of ProKink analysis of CM output vs Prokink analysis of TMH2 in the crystal structure of $\beta$ 2-adrenergic receptor .....	35
Table 4. Comparison of ProKink analysis of CM GPR55 TMH5 output vs Prokink analysis of TMH5 in the crystal structure of $\beta$ 2-adrenergic receptor .....	40
Table 5. Comparison of ProKink analysis of Conformational Memories output vs Prokink analysis of TMH6 in the crystal structure of $\beta$ 2-adrenergic receptor .....	43
Table 6. The correlation of $\chi_1$ of S6.47, F6.44, F6.48 and H6.52.....	44
Table 7. The correlation of $\chi_1$ of F6.48 (239) with F6.44 (235) and H6.52 (243).....	45
Table 8. Comparison of ProKink analysis of CM output vs Prokink analysis of TMH7 in the crystal structure of $\beta$ 2-adrenergic receptor .....	47
Table 9. Correlation of $\chi_1$ of F6.48 (239) with F6.44(235) and H6.52 (243). ....	56

## LIST OF FIGURES

	Page
Figure 1. L- $\alpha$ -Lysophosphatidylinositol (Liver, Bovine-Sodium Salt).....	5
Figure 2. mRNA expression levels of GPR55 and CB1 receptor in mouse tissues measured by quantitative PCR.....	6
Figure 3. General topology of GPCR's.....	11
Figure 4. Torsion angels .....	18
Figure 5. Side chain conformations .....	19
Figure 6. Gauche plus conformation.....	20
Figure 7. Trans conformation .....	20
Figure 8. Gauche minus conformation.....	21
Figure 9. Map of the accessible conformational space as a function of temperature. ....	25
Figure 10. Presence of serine in $\alpha$ Helices .....	28
Figure 11. The structural features of a Pro kink motif that deviate from a standard $\alpha$ - helical conformation are illustrated here.....	29
Figure 12. Illustrates the bend and wobble angle. ....	30
Figure 13. Illustrates the face shift.....	31
Figure 14. Illustrates an example of sequence dictated divergences between CB1 and CB2 receptor .....	32
Figure 15. Primary amino acid sequence of TMH2 in GPR55 and the $\beta$ 2-adrenergic receptor. ....	34
Figure 16. A side view of the 105 TMH2 helices from the CM runs superimposed on TMH2 of the $\beta$ 2-adrenergic receptor is illustrated here. ....	37

Figure 17. Primary amino acid sequence of TMH5 in GPR55 and the $\beta_2$ -adrenergic receptor. ....	39
Figure 18. Illustrated here are side and extracellular views of the 105 TMH5 helices from the CM runs superimposed on TMH5 of the $\beta_2$ -adrenergic receptor...	41
Figure 19. Primary amino acid sequence of TMH6 in GPR55 and the $\beta_2$ -adrenergic receptor. ....	42
Figure 20. Illustrated here are side and extracellular views of the 105 TMH6 helices from CM runs for the GPR55 inactive state superimposed on TMH6 of the $\beta_2$ -adrenergic receptor.....	43
Figure 21. Primary amino acid sequence of TMH7 in GPR55 and the $\beta_2$ -adrenergic receptor. ....	46
Figure 22. Side view of the TMH7 CM output helices superimposed to the ( $\beta_2$ -adrenergic receptor.....	47
Figure 23. Schematic representation of human GPR55 receptor.....	49
Figure 24. Presence of proline causes a distortion of the helical structure.....	52
Figure 25. Ionic lock in GPR55 inactive state .....	54
Figure 26. Toggle switch in GPR55 .....	55
Figure 27. Inactive receptor GPR55 top view (left) and active receptor GPR55 .....	57

## CHAPTER I

### INTRODUCTION

For decades marijuana remains one of the most widely used and abused drug around the world. It interacts with the brain, producing psychoactive and potentially therapeutic effects. Over the past decade it has becoming important to understand the mechanism whereby marijuana interacts in the human body.

Marijuana is the buds and leaves of the *Cannabis sativa* plant. This plant contains more than 400 chemicals, including delta-9-tetrahydrocannabinol (THC), which is the main psychoactive chemical in this plant. THC is known to affect the short term memory, motor coordination, increases heart rate and levels of anxiety.

It has being discovery the existence of naturally occurring marijuana-like substances in the human body. The discovery of specific receptors that are activated by smoking marijuana and the finding of endogenous cannabinoids, which can also activate this receptors have implicated the marijuana-cannabinoid research into mainstream science with important implications in human health and disease.

Cannabinoid receptors are activated by a neurotransmitter called anandamide which belongs to a group of chemicals called cannabinoids, like THC. THC mimics the action of anandamide binding to the cannabinoid receptor and activates the neurons causing adverse effects on the mind and the body.

The cannabinoids have been suggested to play several roles in animals and humans, including the regulation of cell development and growth, modulation of immune function, nervous function, reproductive and feeding behavior, and in a number of biological functions from movement, memory, learning, appetite stimulation, and pain, to emotions, blood pressure, intraocular pressure, etc. The promiscuous action and distribution of cannabinoid receptors in most biological systems provides an extensive signaling capabilities for cross talk between different families of receptors, which may explain the numerous behavioral effects associated with smoking marijuana (1).

At least two subtypes of cannabinoid receptor exist which have been cloned from animal or human source. These subtypes are termed CB1 and CB2. The CB1 receptor is present in the brain with highest density in the hippocampus, cerebellum and striatum. The CB2 receptor is found predominantly in the spleen and in the haemopoietic cells. The existence of this receptor provided the molecular basis for the immunosuppressive actions of marijuana.

Cannabinoid receptors are members of the G-protein coupled receptor (GPCR) super family and mediate inhibition of adenylyl cyclase activity and reduce cyclic AMP levels.

### GPR55

The goal of this research is to determine the structural features of the newly orphanized cannabinoid receptor GPR55 (2,3,4). This receptor belongs to the Class A G-protein-coupled receptor (GPCR) family and binds constituents of the plant, Cannabis

sativa. The CB1 and CB2 receptors were the first cannabinoid receptors discovered. There is biochemical, electrophysiological and behavioral data to suggest that even when the CB1 and CB2 receptors are knocked out (in CB1/CB2 double knockout mice), the endogenous cannabinoid anandamide still produces effects, suggesting the presence of additional cannabinoid receptor subtypes (5).

The ability of GPR55 to recognize CB1 antagonist (SR141716A, Rimonabant) and act as agonist has been reported (2,6). However the aminoalkylindole WIN55,212-2, which is a CB1/CB2 agonist, did not produce an agonist response at GPR55 indicating that this is a distinct receptor from CB1(4,7,8). Palmitoylethanolamide (PEA) has been identified as a potent anti-inflammatory, anti-excitotoxic and anti-hyperalgesic compound, which can act as a endocannabinoid for the GPR55 (4,9,10). Thus GPR55 recognizes many cannabinoids, but has a unique response profile differing from CB1 and CB2. GPR55 exhibits low amino acid identity to CB1 (13.5%) or CB2 (14.4%) receptors. The most closely related proteins to GPR55 are GPR35 (27%), P2Y (29%), GPR23 (30%), and CCR4 (23%) (11).

Ryberg and co-workers have suggested that the role that GPR55 plays in health and disease and any potential therapeutic benefits of activation or blocking of this receptor are yet to be ascertained (12). More recently, the fact that that GPR55 signaling can influence the regulation of certain cytokines has led to the hypothesis that GPR55 may contribute to the lack of inflammatory mechanical hyperalgesia in the GPR55<sup>-/-</sup> (knockout) mice. Consequently, it has been suggested that the manipulation of GPR55

may have therapeutic potential in the treatment of inflammatory and neuropathic pain (13).

Two receptors for anandamide were found in human endothelial cells, characterized as cannabinoid 1 receptor (CNR1) and G-protein-coupled receptor 55 (GPR55). Both receptors trigger distinct signaling pathways upon anandamide stimulation where the integrins are activated and the signaling cascade becomes promoted. It has been reported that the effect of anandamide on endothelial cells depends on the status of the integrin clustering (14).

GPR55 is highly expressed in larger dorsal root ganglion neurons and upon activation by various cannabinoids ( $\Delta^9$ THC, the anandamide analog R-methanandamide and JWH015) increases intracellular calcium in these neurons. The signaling pathways involved in HEK293 cells expressing GPR55 which lead to an increase of calcium involves  $G_q$ ,  $G_{12}$ , RhoA, actin, phospholipase C, and calcium released from  $IP_3$ -R gates stores. These pathways are quite different from those used by CB1 and CB2 (15).

Lysophosphatidylinositol (LPA) has been reported to be a possible endogenous ligand for GPR55 (see Figure 1). In HEK293 cells expressing GPR55, LPA produces a rapid  $Ca^{2+}$  transient signal and stimulation of GTP $\gamma$ S(16). Pertwee and co-workers reported that both the CB1 receptor antagonist, AM251 and the CB1/CB2 agonist,  $\Delta^9$ THC are able to activate GPR55. In addition, the CB1 endogenous antagonist virodhamine and non-CB1/CB2 ethanolamides, palmitoylethanolamide and

oleoylethanolamide activate GPR55 by coupling with  $G\alpha_{13}$  (16). Information about additional GPR55 ligands is summarized in Table 1.

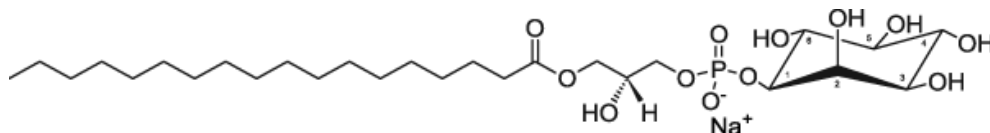


Figure 1. L- $\alpha$ -Lysophosphatidylinositol (Liver, Bovine-Sodium Salt)

Pertwee and co-workers also compared the distribution of GPR55 and CB1 mRNA in mouse (16) (see figure 2). The results of the expression profile of GPR55 in a panel of mouse tissue using PCR showed the presence of GPR55 mRNA with high levels in the adrenals, parts of the gastrointestinal tract and the CNS. Similar to CB1, GPR55 has a broad distribution in brain tissue but the levels are significantly lower than those for CB1(16).



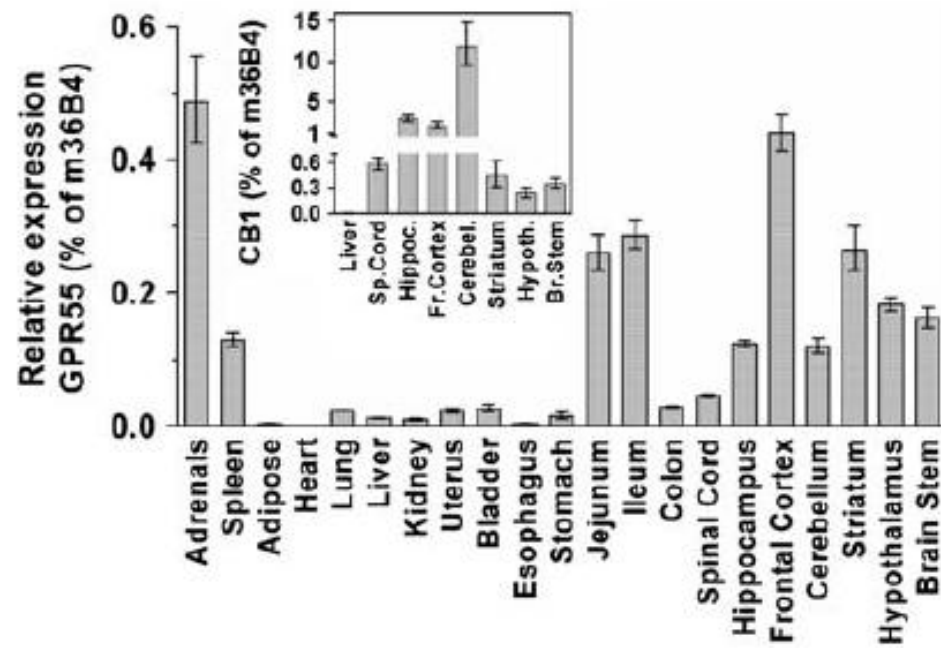


Figure 2. mRNA expression levels of GPR55 and CB1 receptor in mouse tissues measured by quantitative PCR. Data are mean values  $\pm$  s.e.m. using tissue from eight (GPR55) or four mice (CB1).

Table 1. Comparative table of the different GPR55 ligands.

<b>The orphan receptor GPR55 is a novel cannabinoid receptor (E. Ryber et al, September 17<sup>th</sup>, 2007)</b>	<b>Identification of GPR55 as a lysophosphatidylinositol receptor (Saori Oka et al., August 24<sup>th</sup>, 2007)</b>	<b>The GPR55 ligand L-<math>\alpha</math>-lysophosphatidylinositol promotes RhoA-dependent Ca<sup>2+</sup> signaling and NAFT activation (Henstridge C., et al August 29<sup>th</sup>, 2008)</b>
<i>Expression profiling</i>		
Mouse tissues using PCR -adrenals -Part of intestinal tract -CNS But levels are lower than CB1		
<i>Radioligand binding assay</i>		
-specific binding for CP55940 -small specific binding for SR141716 -no binding for WIN55,212-2		
<i>ERK phosphorylation</i>		
	2AG, anandamide, PEA, N-oleoylethanolamide, virhodamide, CP55940, HU210, WIN55,212-2, - $\Delta^9$ THC, abnormal cannabidiol, and SR141716 did not exert any effect -LPI induced a rapid phosphorylation of ERK cell expressing GPR55	
<i>GPR55 cellular localization</i>		
		-LPI was capable of inducing receptor internalization from the plasma membrane to the intracellular vesicles
<i>[<sup>35</sup>S] GTP<math>\gamma</math>S binding assay</i>		
-CP55940 increased GTP $\gamma$ S binding with EC <sub>50</sub> 18 nM -2-AG, noladin ether, PEA, virodhamine	-LPI dose dependently stimulated the binding of [ <sup>35</sup> S] GTP $\gamma$ S to the GPR55 expressing cell	

and OEA stimulated GTP $\gamma$ S binding - $\Delta^9$ THC, HU210 AM251 stimulated binding -cannabidiol antagonize the agonist effect of CP55940 -WIN55,212-2 and AM281 no functional activity	membranes	
<i>G protein coupling</i>		
-No effect Pertussis toxin      no Gi -No calcium signaling      no Gq -G $_{13}$ present GTP $\gamma$ S binding in a dose dependent manner		-LPI mediated Ca $^{2+}$ signaling involving G $\alpha$ 13
<i>Evaluation of LPI on Ca<math>^{2+}</math> homeostasis in GPR55 –HEK293 cells</i>		
	30 nM of LPI provoked a Ca $^{2+}$ transient in GPR55-expressing cells	-Exposure to LPI resulted in a concentration dependent induction of oscillating Ca $^{2+}$ -LPI evokes Ca $^{2+}$ released from intracellular stores
<i>Ability of GPR55 to induce NFAT (Ca<math>^{2+}</math>/ calcineurin dependent regulator of transcription)</i>		
		Treatment of cells with an increased amount of LPI resulted in a dose dependent induction of NFAT activity
<i>Downstream signaling by GPR55</i>		
-Anandamide and 01602 but not WIN55,212-2 induced activation of rhoA, cdc42 and rac1 -Effect was blocked by cannabidiol		-RhoA is a downstream effector of G $\alpha$ 12/G $\alpha$ 13 family -1 $\mu$ M of LPI elicited RhoA activation
<i>Do cannabinoids promote GPR55- mediated Ca<math>^{2+}</math> signaling? (profile of activity of selected cannabinoids ligands in GPR55-HEK293 cells using Ca<math>^{2+}</math> signaling as a reporter of receptor activity)</i>		
		-AEA and 2-AG were able to elevate intracellular Ca $^{2+}$ levels in a concentration range of 3-30 $\mu$ M -but not difference in maximal response, duration and potency were observed compared to the control

		-CP55940 had no effect on intracellular $\text{Ca}^{2+}$ levels -AM251 was able to induce sustained $\text{Ca}^{2+}$ response but it was less potent than LPI
<i>Remarks</i>		
-vascular tone-controlling receptor -inflammatory activities	-LPI is an acidic lysophospholipid -LPI is a possible degradation product of phosphatidylinositol -LPI reduced the response induced by the subsequent stimulation with LPI, suggesting desensitization in LPI pretreated cells -levels of LPI in patient with ovarian cancer was markedly higher -LPI may stimulate the growth and metastasis of ovarian cancer	-Characteristic of GPR55 are unique a) no other GPR55 links the signaling pathways of $\text{G}\alpha_{13}$ and small G-TPases like RhoA b) with oscillatory and prolonged $\text{Ca}^{2+}$ signaling c) and downstream NFAT activation which can regulate DNA transcription and gene expression -LPI can activate GPR55 -but endocannabinoids AEA and 2-AG have not clear effect at equivalent concentrations -GPR55 knockout animals data suggest a potential role within the brain, neurons and immune cells regulating inflammatory/neuropathic pain -LPI is known to have mitogenic activity and may influence the growth of certain tumors

## GPCR Structure and Function

GPCRs are transmembrane proteins that serve as a link to cellular signal transduction mechanisms. Due to the technical difficulties associated with crystallizing transmembrane proteins such as GPCRs, only a few GPCRs have been crystallized to date. These include rhodopsin (17,18,19), the beta-2-adrenergic receptor ( $\beta$ 2-AR)(Cherezov et al., 2007; Rasmussen et al., 2007; Rosenbaum et al., 2007),  $\beta$ 1-AR (Warne et al., 2008), and adenosine A2A receptor (Jaakola et al., 2008). Rhodopsin is the prototypical Class A GPCR and its crystal structure represents the dark-adapted (inactive state) (17,18,19). It has been used as the basis for homology modeling of other Class A GPCRs. The general topology for the GPCRs include: an extracellular N terminus seven transmembrane (TM) alpha helices arranged to form a closed bundle; loops that extend intra- and extracellularly connecting TM helices an intracellular C terminus that begins with a short helical segment (helix 8) oriented parallel to the membrane surface.

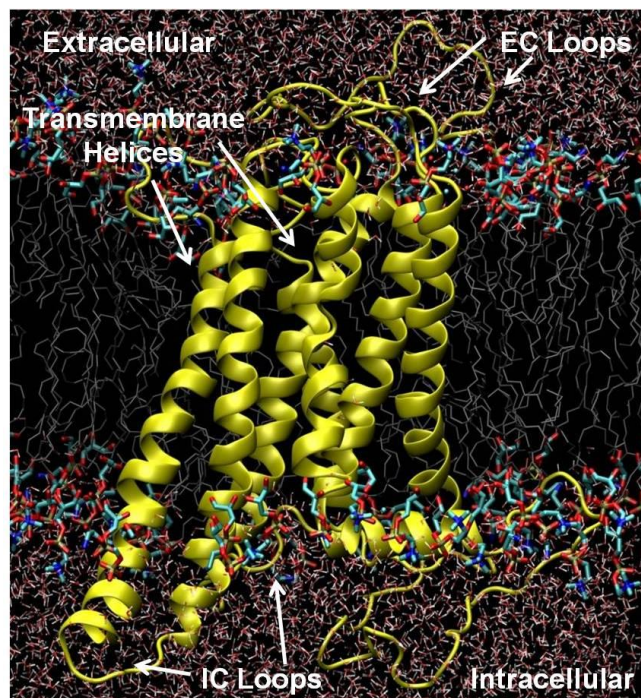


Figure 3. General topology of GPCR's.

Ligand binding is thought to occur within the binding site crevice formed by the transmembrane helix (TMH) bundle, to extracellular loops, or to a combination of extracellular loop and binding site crevice residues. The homology models developed in the Reggio lab for the CB1 and CB2 receptors have been modified based on sequence dictated divergences between rhodopsin and each cannabinoid receptor subtype. These models have been very successful in identifying key interaction sites for classical cannabinoids (**20**), non-classical cannabinoids (**21**), aminoalkylindoles (**22**) and biarylpyrazoles (**23**).

The primary structural information about GPCR activation comes from biophysical studies of rhodopsin and the  $\beta$ 2-adrenergic receptor ( $\beta$ 2-AR). These studies

indicate that the rotation of both TMH 3 and TMH 6, as well as a conformational change in TMH 6 (straightening in the CWXP hinge region of the TMH6) occurs upon GPCR activation (24,25,26,27,28,29). The time scale for the activation of the  $\beta$ 2-AR by its diffusible ligand has been reported as seconds (25). This has been shown to be true in live cells, as well (29). This time scale is quite long compared to the typical length of molecular dynamics (MD) simulations (10- 100 ns). For this reason different models of the active states of CB1/CB2 (22,30) and GPR35/55 had been created based on documented changes that occur during the activation process. Light activation of rhodopsin does not require the breaking and forming of thousand of specific contacts within nanoseconds, only specific contacts restricting the inactive state are broken during activation. These changes are then transmitted through the entire membrane protein because of its dynamic plasticity. It has been reported that a key tryptophan residue in the ligand binding pocket, W6.48(265) is restricted in rhodopsin. In the dark (inactive) state of rhodopsin, the beta-ionone ring of its covalently bound ligand, 11-cis-retinal is close to W6.48(265) of the CWXP motif on TMH F and helps constrain it in a  $\chi_1 = g^+$  conformation (17,18,19). In the presence of light, this receptor activates and the beta-ionone ring moves away from TMH F and toward TMH D where it resides close to A4.58(169) (31). During this process the constraint on W6.48(265) is released, making it possible for W6.48(265) to undergo a conformational change. This suggests that the conformation of W6.48 (265) when rhodopsin is inactive (R;  $\chi_1 = g^+$ ) changes during activation to a trans conformation ( $\chi_1 g^+ \rightarrow \text{trans}$ ) (32). Another interaction that has been reported as important is W6.48/F3.36 which may act as the “toggle switch” for

CB1 activation, with W6.48  $\chi_1$  g+ /F3.36  $\chi_1$  trans representing the inactive state (R) and W6.48  $\chi_1$  trans /F3.36  $\chi_1$  g+ representing the active state (R\*) state of CB1 (33). It has been suggested that F3.36 may restrain W6.48 from moving to an activated state conformation (34).

Table 2: Summary of GPCR Activation

GPCR ACTIVATION	
Inactive (R) State	Active (R*) State
W6.48 $\chi_1$ in g+ (-60°) N – C $\alpha$ – C $\beta$ – X	W6.48 $\chi_1$ in trans (180°) N – C $\alpha$ – C $\beta$ – X
“Ionic lock”: Rho: Arg 3.50 & Glu 6.30	“Ionic lock” broken: TMH3/6 Rotate
Toggle Switch ( $\beta$ 2-AR) C6.47/W6.48/F6.52 trans g+ g+	Toggle Switch ( $\beta$ 2-AR) C6.47/W6.48/F6.52 g+ trans trans

To build the activated state model of GPR55 we used the biophysical literature on the R to R\* transition in Class A GPCRs, such as rhodopsin and  $\beta$ 2-adrenergic receptor. This literature suggests that activation is accompanied by a straightening of the TMH 6 and rotation of TMH 3 and TMH 6. The identity of the residue 6.49 can have a profound effect on the flexibility of TMH 6 (35) GPR55 like rhodopsin has a Leu at position 6.49. To generate an activated model of GPR55 we selected a conformer for which the proline kink angle is moderated as compared to the TMH 6 conformation in the rhodopsin crystal



structure (19). TMH 6 was also rotated so that Cys 6.47 becomes accessible from inside the binding site crevice (27). TMH 3 was rotated so that residue 3.41 changes environments (26). We expect that the most significant changes in the R to R\* transition will be seen in the binding pocket of GPR55 due to the change of residue accessibilities on TMH6. The groove residues V6.43/V6.46 will rotate to the TMH6/7 interface, S6.47 will become accessible to the ligand binding pocket. And H6.52 and F6.59 will rotate out of the binding pocket.

In the present research, the amino acid numbering sequence to be used is the one proposed by Ballesteros and Weinstein (36). In this numbering system, the most highly conserved residue in each transmembrane helix (TMH) is assigned a locant of 0.50. This number is preceded by the TMH number and may be followed in parentheses by the sequence number. All other residues in a TMH are numbered relative to this residue. The sequence numbers used here are from human GPR55 (37). In the Ballesteros-Weinstein numbering system, for example, the most highly conserved residue in TMH 2 of the GPR55 receptor is D2.50(70). The residue that immediately precedes it is called F2.49(69). Residues in the intracellular extension of TMH 7 are numbered as if they are part of TMH7 following the literature precedent set by Prioleau and co-workers (38). Among the highly conserved residues typically used in sequence alignments with rhodopsin, GPR55 has the conserved patterns in TMH1, 2, 4 and 5 (i.e. N1.50, D2.50, W4.50, and P5.50). The fact that CB1 and CB2 lack the highly conserved P5.50 while GPR55 has this motif, suggests a structural divergence in TMH5 between CB1/CB2 and GPR55. GPR55 has the substitution DRF for the conserved TMH3 E/DRY motif in

CB1/CB2. In TMH6, the highly conserved CWXP motif found in rhodopsin and CB1/CB2 is substituted with SFLP in GPR55. The greatest divergence from the rhodopsin sequence and from CB1 and CB2 appears in THM7 because the highly conserved NPXXY motif is replaced with DVFCY (GPR55). Like rhodopsin, GPR55 has an F in the intracellular extension of TMH7 (called Hx8) at position 7.60. In rhodopsin, there is an aromatic interaction between Y7.53 (306) and F7.60 (313), which has been proposed to provide structural constraints that rearrange in response to photoisomerization (39). In GPR55, the analogous relationship between Y7.53 and F7.60 can be established, but this interaction is not possible in CB1/CB2 because at position 7.60 there is Leu in CB1 and Ile in CB2.

GPR55 also potentially has another significant similarity to rhodopsin in its EC-2 loop structure. In rhodopsin, the EC-2 loop dips down into the binding pocket to form a disulfide bridge between an EC-2 Cys residue and C3.25. It then loops back over itself to make its connection with the top of TMH5. GPR55 has a Cys at 3.25 and a Cys residue in the EC-2 loop that could potentially form a disulfide bond. It is likely that EC-2 loop structure of GPR55 will differ from that of CB1 and CB2 as these latter receptors lack the Cys at position 3.25.

The initial model for GPR55 built in the Reggio lab was based upon a rhodopsin template. Work with CB1 and CB2 has shown that although the rhodopsin crystal structure is a good starting point for cannabinoid receptor modeling, there are sequence dictated differences between rhodopsin and each of these receptors that can result in local divergence from the rhodopsin structure. These can be manifested by the absence of a

key motif, by divergent locations of proline or glycine residues, as well as by the presence of serines or threonines in key positions that can exert subtle, but important effects upon helix conformation.

## CHAPTER II

### OBJECTIVE

The objective of my thesis is to use the biased Monte Carlo/simulated annealing method, Conformational Memories (CM) to refine the transmembrane helix (TMH) conformations of TMHs in GPR55 that have significant sequence divergences from other Class A GPCRs. These include TMH2, TMH5, TMH6 and TMH7 of GPR55. The result of these calculations will be used to modify the GPR55 computer model initially built in the Reggio lab based on a rhodopsin template to generate refined R and R\* models for GPR55.

## CHAPTER III

### METHODS

#### Molecular Modeling

Definition of torsion angles

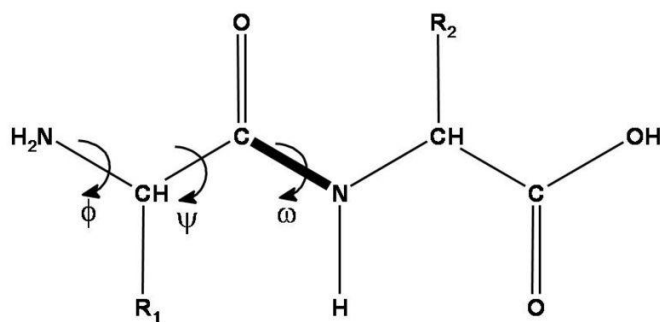


Figure 4. Torsion angles

Dihedral angle  $\phi$  : rotation about the bond between N and  $\text{C}_{\alpha}$  bond, involves  $\text{C}(\text{O})-\text{N}-\text{C}_{\alpha}-\text{C}(\text{O})$

Dihedral angle  $\psi$  : rotation about the bond between  $\text{C}_{\alpha}-\text{C}(\text{O})$  bond involves  $\text{N}-\text{C}_{\alpha}-\text{C}(\text{O})-\text{N}$

Dihedral angle  $\omega$  : rotation about the peptide bond  $\text{C}(\text{O})-\text{N}$  bond involves  $\text{C}_{\alpha 1}-\text{C}(\text{O})-\text{N}-\text{C}_{\alpha 2}$

$\omega$  angle tends to be planar ( $0^\circ$  - cis, or  $180^\circ$  - trans) due to delocalization of carbonyl pi electrons and nitrogen lone pair

$\phi$  and  $\psi$  are flexible, therefore rotation occurs here

### Side chain conformation

The Greek alphabet is used to name the side chain atoms of the amino acids according to this scheme.

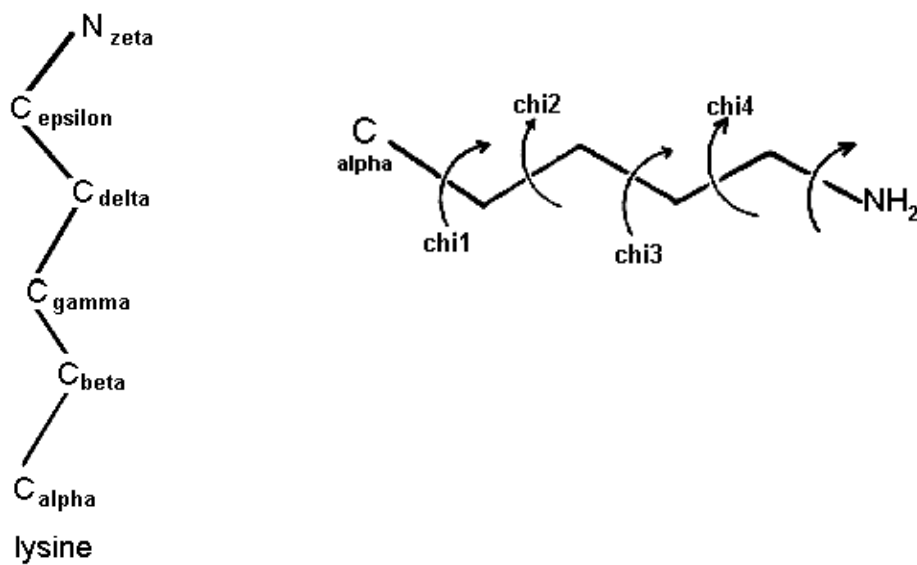


Figure 5. Side chain conformations.

The side chain torsion angles are named  $\phi$ 1( $\chi$ 1),  $\phi$ 2( $\chi$ 2),  $\phi$ 3 ( $\chi$ 3), *etc.*,

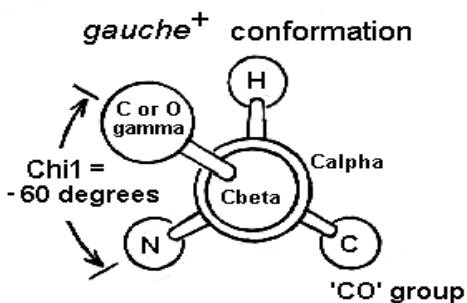


Figure 6. *Gauche plus* conformation

The most abundant conformation is *gauche*(+) in which the gamma side chain atom is opposite to the residue's main chain carbonyl group when viewed along the C $\beta$ -C $\alpha$  bond.

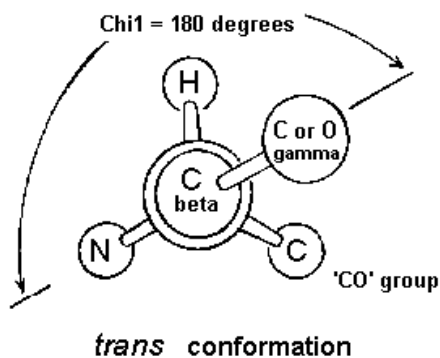


Figure 7. *Trans* conformation.

The second most abundant conformation is *trans* in which the side chain gamma atom is opposite the main chain nitrogen.

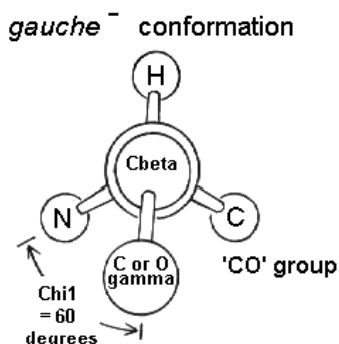


Figure 8. Gauche minus conformation

The least abundant conformation is *gauche(-)*. Occurs when the side chain is opposite the hydrogen substituent on the C  $\alpha$  atom. This conformation is unstable because the gamma atom is in close contact with the main chain CO and NH groups. The *gauche(-)* conformation is occasionally adopted by serine or threonine residues in a helix where the steric hindrance is offset by a hydrogen bond between the gamma oxygen atom and the main chain.

#### Models of TMH 2, TMH 5, TMH 6 and TMH 7 for GPR55

Low free energy helix conformations for GPR55 TMH2, TMH5, TMH6 and TMH7 were created using the conformational memories (CM) technique to explore the sequence dictated conformations of these key helices. In most cases, the helix was built using the standard  $\phi$  ( $-63^\circ$ ) and  $\psi$  ( $-41.6^\circ$ ) backbone dihedrals for TM helices (Ballesteros



and Weinstein 1995) (36). Backbone phi and psi torsion angles were allowed to vary by  $\pm 10^\circ$ , with a larger variation ( $\pm 50^\circ$ ) used in more flexible regions of the helix, i.e. those containing known helix bending residues, such as proline, glycine, serine or threonine (40). Side chain torsions were allowed to vary  $\pm 180^\circ$ , unless otherwise specified. The protocol for bond angle variation will be discussed below.

**TMH2 Flexible Region:** TMH2 in Rho does not have a proline, however it does have helix distortion from G2.56 to T2.59 (GGFT). GPR55 lacks this GGFT sequence, but it has a proline at 2.58. It is possible that this proline is a structural mimic of GGFT. In CM calculations, the region from V2.54 to P2.58 was considered to be the flexible region in GPR55 TMH2. S2.56 near P2.58 was set to be in g minus  $\chi_1$  exploring this region and this helix will be build based on the backbone of the  $\beta_2$  adrenergic receptor conformation for the proline kink.

**TMH5:** In Rhodopsin and the  $\beta_2$  adrenergic receptor, there is a single proline residue in TMH5 at position 5.50, which causes a deviation from normal alpha-helicity in the region, 5.46-5.50. TMH5 in GPR55 has two proline residues (P5.41 and P5.50) which could cause distortions from normal alpha-helicity. GPR55 TMH5 was built based on the backbone of the  $\beta_2$  adrenergic receptor in order to capture the helix distortion around P5.50. The region from K5.37 to P5.41 was then considered flexible in CM calculations.

**TMH6:** TMH6 in GPR55 does not have the Class A GPCR highly conserved CWXP motif. However, it has the conservative substitutions of this motif: SFLP. Since TMH6 has been implicated in conformational changes during receptor activation (24,25,26,27,28,29), it was very important to study the allowed conformations of GPR55

TMH6. Results from these studies were used to build not only the inactive state model of GPR55, but also the activated state model. CM calculations for TMH6 considered the region from V6.46 to P6.50 to be flexible in GPR55. The residue serine 6.47 was run under two conditions. In the first condition, the S6.47  $\chi_1$  was not restricted. In the second condition, the S6.47  $\chi_1$  was held in trans position due to its position and possible structural role found by Juan Ballesteros (36).

**TMH7:** TMH7 in Class A GPCRs usually has the conserved sequence motif, NPXXY, which not only influences the conformation of TMH7, but also places Y7.53 in the correct position to interact with F7.60 on the intracellular extension of TMH7, Hx8. GPR55 lacks the NPXXY motif in TMH7. Instead, this region of the sequence is DVFCY in GPR55. The CM protocol for CB1 in TMH7 calls for the region from S7.46 to P7.50 to be considered the flexible region of TMH7. To parallel this, the span from C7.46 to V7.50 (GPR55) was considered to be the flexible region.

#### Conformational Memories (CM)

In order to explore the different conformation of the helices TM2, TM5, TM6 and TM7 the conformational memories (CM) method was used. This method employs multiple Monte Carlo/simulated annealing random walks and the CHARMM 32 force field (41). The CM method is widely used because it converges in a very practical number of steps and it is capable of overcoming energy barriers efficiently. The CM method can fully characterize the conformational properties of a helix by the free energy of each of the conformations that the helix can adopt, which includes not only the intrinsic energy of each conformational state, but also the probability that the helix will

adopt each particular conformation relative to all other ones accessible in an equilibrated thermodynamic environment. The calculations are performed in two phases. In the first phase repeated runs of Monte Carlo/simulated annealing are carried out to map the entire conformational space of the helix. The dihedral and bond angle space in which conformations were accepted are used to create “memories”. In the second phase, new Monte Carlo/simulated annealing runs are performed only in the populated regions (“memories”) identified in the first phase of the calculation. All calculations are run using a distance dependent dielectric.

The two phases are described in more detail below:

#### Exploratory phase

In the exploratory phase of the CM method, a random walk is used to identify the region of conformational space most probable for each torsion angle and bond angle. The initial temperature for each run is 3000 K with 50,000 Monte Carlo steps applied to each torsion or bond angle variation with cooling in 18 steps to a final temperature of 310 K. Each step consists of varying two dihedrals angles and one bond angle chosen at random from the entire set of variable angles. The torsion angles and bond angles are randomly picked at each temperature and each move is accepted or rejected using the Metropolis criterion (30). Accepted conformations in the Exploratory Phase are used to create “memories” of torsion angles and bond angles that were accepted. This information provides a map of the accessible conformational space of each TMH as a function of temperature.

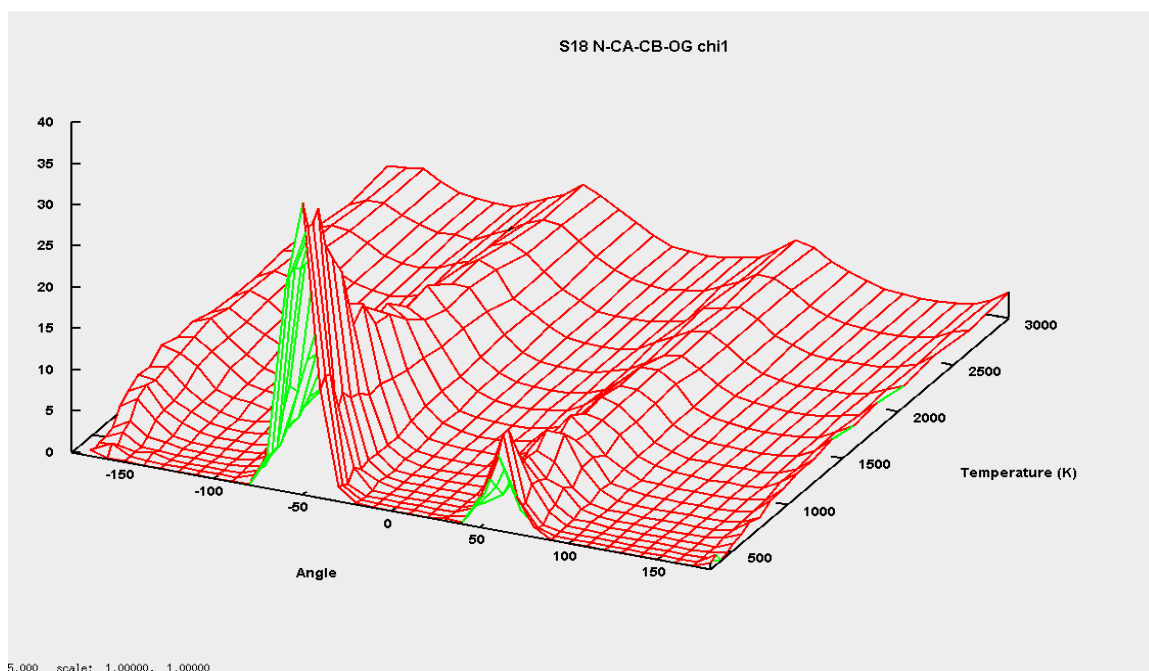


Figure 9. Map of the accessible conformational space as a function of temperature. CM Map of S4.54 Chi1 Pre-biased (Exploratory) Phase.

### Biased annealing phase

In the second phase of the CM calculations, the only torsion angles and bond angles moves attempted are those that would keep the angle in the “populated conformational space” mapped in the exploratory phase. The biased annealing phase began at 749.4 K cooling to 310 K in 7 steps. Finally, 105 structures were output at 310 K for each TMH.

### Metropolis criterion

In the metropolis criterion or algorithm the first conformation is randomly generated and each point in the construction of the conformation a move is attempted to

the current conformation. If the local chain conformation is not compatible with the attempted move then the movement is rejected immediately. If the conditions are satisfied then the metropolis criterion is applied. The acceptance probability (P) of a trial move is chosen to be

$$P = \min(1; \exp(-\beta \cdot \Delta E))$$

where  $\beta = 1/T$ .

#### Variable bond angles

The memories for bond angles are defined in the range 90° to 144° with 1.5° bin sizes, using pre-biased memories for all bond angles to avoid sampling high energy regions of bond angle space. The bonds angles present in aromatic rings and side chain bond angles that include non polar hydrogens are not varied. The other angles are allowed to vary in a range of  $\pm 8^\circ$  around the initial value. Bond angles involving polar hydrogens or the C-S-C angles are allowed to vary up to  $\pm 15^\circ$  around the initial value. The full set of bond angles and dihedrals angles of a molecule determines the molecular structure and using the internal coordinates of CHARMM, the minimum set of bond angles necessary to construct the coordinates of the system are determined.

#### Evaluation of CM Output

***Helix Geometry.*** The average proline kink angle and standard deviation for each set of conformational results generated by CM were measured using the ProKink program (40). This program, which is part of Simulaid Conversion program was used to calculate the face shift, wobble angle, and bend angle of each helix. A statistical analysis

of the resultant face shift, wobble angle and bend angle for the 105 helices was performed using the statistical analysis package (GraphPad Software for one sample t test).

#### Helix Choice for TMH Bundle.

The 105 helices output for each run were superimposed on the appropriate helix in the beta-2 adrenergic receptor template. For TMHs 2,5, 7 and the TMH6 inactive state, output helices were superimposed from the intracellular side up to (but not including) the flexible region. For the TMH6 activated state, CM output was superimposed from the extracellular end up to (but not including) the flexible region. For all helices except TMH6, helices were chosen based upon their fit within the TMH bundle. The helix chosen for the TMH6 inactive state was chosen for fit and also for its ability to form an R3.50/Q6.30 interaction. The helix chosen for the activated state of TMH6 was chosen such that this interaction was broken. Additional criteria used for helix selection will be discussed in the Results section.

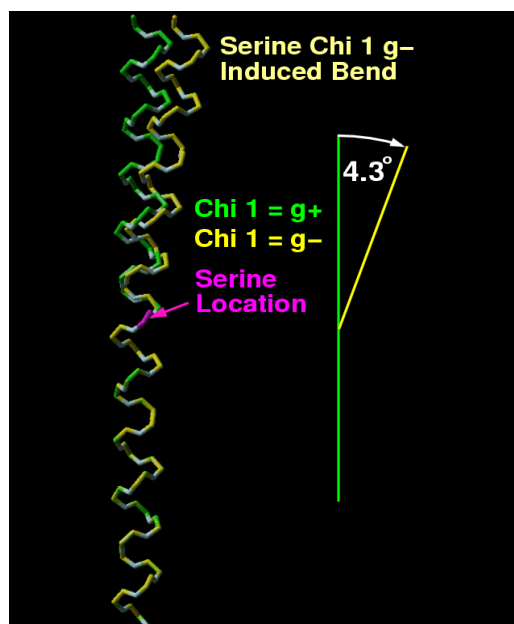


Figure 10. Presence of serine in  $\alpha$  Helices

Ballesteros et. al., documented the effects of Serine residues found in a  $g^-$  or  $+60^\circ$  where the hydrogen bonding to the  $i-3$  carbonyl oxygen of the backbone could bend the  $\alpha$  helix creating an angle of  $4.3^\circ$ . Ballesteros et. al. Ref Ballesteros J.A., Deupi X., Olivella M., Haaksma E.E.J. and Pardo L. Serine and threonine residues bend  $\alpha$ - helices in the  $\chi_1 = g^-$  Conformation. Biophysical Journal Volume 79 November 2000-2754-2760

#### Presence of proline in $\alpha$ Helices

It is known that the presence of proline residues in  $\alpha$ -helices can perturb the structure by introducing a kink between the segments preceding and following the proline residues. The distortion of this helical structure is the result of the avoided steric clash between the ring of the proline at position (i) and the backbone carbonyl at position (i-4),

as well as the elimination of helix backbone H-bonds for the carbonyls at position (i-3) and (i-4). Figure 12 shows an example of the structural features of a proline kink.

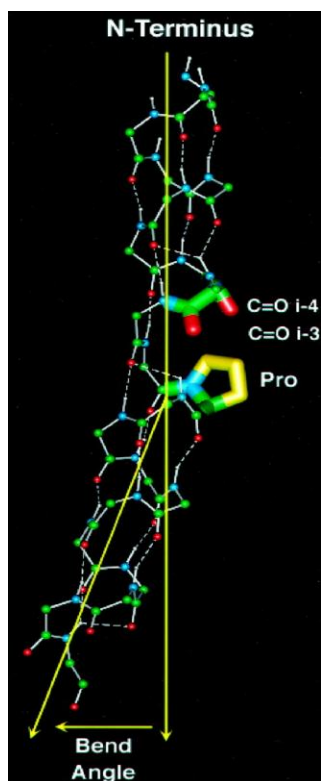


Figure 11. The structural features of a Pro kink motif that deviate from a standard  $\alpha$ -helical conformation are illustrated here.

The Pro residue (yellow) induces a bend in the  $\alpha$ -helix, defined as the angle between the axes (yellow) of the helical segments preceding the Pro kink and following it. The opening of the helix backbone induced by the Pro residue results in an increased solvent accessibility for the carbonyls of amino acids located at positions  $I - 3$  and  $I - 4$  from the Pro. The hydrogen bonding pattern of the  $\alpha$ -helix is broken in the Pro kink



motif: the carbonyls of amino acids located at positions  $I - 3$  and  $I - 4$  from the Pro are not hydrogen bonded.

### Bend angle and wobble angle definition

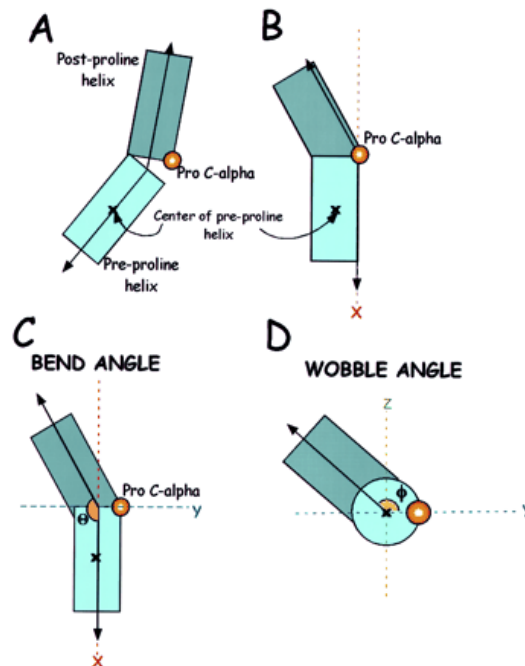


Figure 12. Illustrates the bend and wobble angle.

**Bend angle:** Angle between the two parts when the helix is kinked along its axis.

**Wobble angle:** Angle that defines the orientation of the post-proline helix in three dimensional space, with respect to the pre-proline helix.

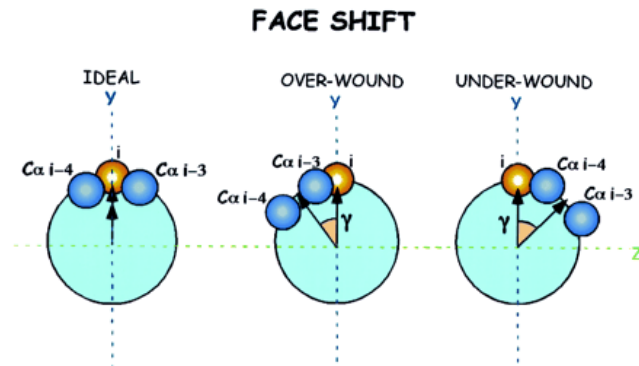
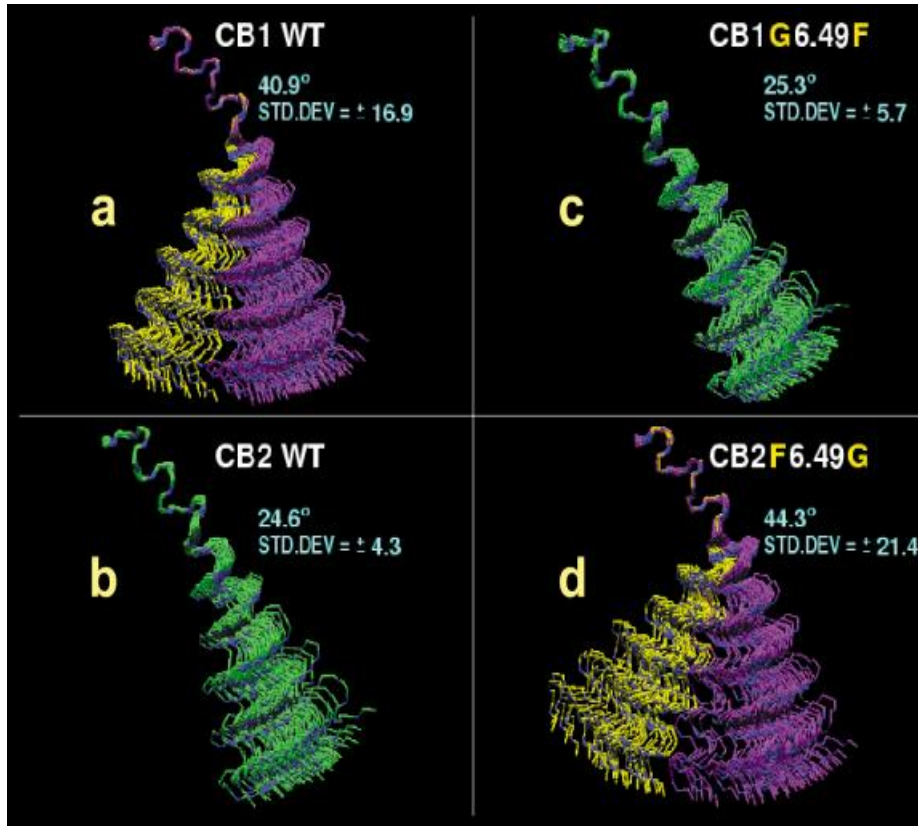


Figure 13. Illustrates the face shift.

**Face shift:** Measures the distortion that causes a twist of the helix “face” in such a way that amino acids that used to be on the same side (face) of the helix are shifted and are on a different side as a results of presence of the proline bend

## Sequence Dictated Divergence



CB1 TMH6 DIRLA<sup>6</sup>KT<sup>6</sup>LV<sup>6</sup>LILV<sup>6</sup>LI<sup>6</sup>IC<sup>6</sup>W<sup>6</sup>G<sup>6</sup>P<sup>6</sup>LLA<sup>6</sup>IMVYDVFG

CB2 TMH6 DVRLA<sup>6</sup>KT<sup>6</sup>LG<sup>6</sup>LV<sup>6</sup>LAV<sup>6</sup>LL<sup>6</sup>IC<sup>6</sup>W<sup>6</sup>F<sup>6</sup>P<sup>6</sup>VLALMAHSLAT

Figure 14. Illustrates an example of sequence dictated divergences between CB1 and CB2 receptor.

An example of sequence dictated divergences is the study of TMH6 in CB1/CB2 where the residue 6.49 preceding P6.50 of motif CWXP between CB1 and CB2 is G6.49 for CB1 and F6.49 for CB2. The conformational memories for CB1 TMH6 showed a

wider range of kink angles than CB2. But when the mutants were switched as shown in figure 15, CB2 showed the same angles of kink.

#### R and R\* Model Refinement

Revised versions of TMHs 2, 5, 6 and 7 that result from CM studies were substituted for the existing helix in the GPR55 model. The OPLS\_2005 all atom force field in Macromodel 9.1 (Schrödinger, LLC, New York, NY, 2005) was used to energy minimize the GPR55 R and R\* models. An 8.0 Å extended non-bonded cutoff (updated every 10 steps), 20.0 Å electrostatic cutoff, and 4.0 Å hydrogen bond cutoff was used in each stage of the calculation and the energy was minimized until an energy gradient of 0.1 kcal/mol is reached.

Loops affected by the replacement of TMH2 ((IC-1,EC-1), TMH5 (EC-2, IC-3)), TMH6(IC-3,EC-3) and TMH7 (EC-3) were modeled using the Modeller program (42,43).

## CHAPTER IV

### RESULTS

#### TMH2

Conformational memories (CM) calculations on TMH2 of GPR55 were used to explore the accessible conformation of TMH2. The average proline kink angle and standard deviation for each set of conformational results generated by CM were measured using the ProKink program (40). This program, which is part of Simulaid Conversion program was used to calculate the face shift, wobble angle, and bend angle of each helix. A statistical analysis of the resultant face shift, wobble angle and bend angle for the 105 helices containing the proline at position 2.58 (78) was performed using the statistical analysis package (GraphPad Software for one sample t test) and compared to TMH2 of the  $\beta_2$ -adrenergic receptor which contains a proline at position 2.59. Figure 15 illustrates the primary amino acid sequence of TMH2 in GPR55 vs. the  $\beta_2$ -adrenergic receptor.

Helix 2 sequence	
	2 2
	5 5
	8 9
GPR55	ATSIYMINLAVFDLLLVL <b>SL</b> PFKMVLSQVQ
Beta-2	VTNYFITSLACADLVMGLAVV <b>PF</b> GAAHILM

Figure 15. Primary amino acid sequence of TMH2 in GPR55 and the  $\beta_2$ -adrenergic receptor.

We expected that the presence of proline residues and the different position of this residue in the Beta 2 receptor and GPR55 (Beta 2 has proline at 2.59 but GPR55 has proline at 2.58) can perturb the helical structure and give a different conformation of TMH2.

We considered the region from V2.54 to P2.58 as flexible helix regions and serine 2.56 near the Proline 2.58 was set in g- position for  $\chi_1$  torsion angle

A one sample independent t test was used to analyze the means of the bend angle, wobble angle, and face shift for the GPR55 CM results containing P2.58 (78) compared to the crystal structure of  $\beta_2$ -adrenergic receptor (containing P2.59). This test revealed that, at the p=0.05 level, the difference of the population means of GPR55 CM results bend angle and face shift were significantly different from TMH2 in the crystal structure of  $\beta_2$ -adrenergic receptor. No statistically significant difference was found for the wobble angle between GPR55 TMH2 CM results and TMH2 in crystal structure of  $\beta_2$ -adrenergic receptor. Results are shown in Table 3.

Table 3. Comparison of ProKink analysis of CM output vs Prokink analysis of TMH2 in the crystal structure of  $\beta_2$ -adrenergic receptor

Proline Position	Bend Angle (degrees)	Face Shift (degrees)	Wobble Angle (degrees)
<b>P 2.59</b> ( $\beta_2$ -adrenergic)	<b>17</b>	<b>95.4</b>	<b>-83.3</b>
<b>*P 2.58 (GPR55)</b>	<b>**39.2 <math>\pm</math> 8.5</b>	<b>**77.9 <math>\pm</math> 30.7</b>	<b>-79.1 <math>\pm</math> 45.4</b>

\*Values are presented as mean  $\pm$  S.D.

\*\* Statistically significant difference at P 0.05 level in one-sample independent t test.

The 105 helices from the CM output were superimposed from A2.38 (58) to L2.53 (73) to compare the populations of TMH2s. In the context of a three dimensional model of the GPR55 receptor, the criteria used to identify a TMH2 helix for bundle incorporation were:

The helix must conserve the interaction between residue D2.50 (70) and D7.49 (284) such that a water molecule could connect these two residues (analogous to the key interaction observed in Rho).

The helix must have no van der Waals overlaps with other TM helices in the bundle. The extracellular end of TMH2 must be close enough to the extracellular end of TMH3 to meet a distance criterion based upon the extracellular loop -1 (EC-1) length. The GPR55 EC-1 loop (SPF) contains half of the number of residues as Rho (GYFVFG). The attachment of EC-1 loop must be possible without over tightening the TMH backbone that would cause van der Waals overlaps.

The resultant superposition with the CM results superpositioned to the beta-2 adrenergic receptor is shown in figure 16.

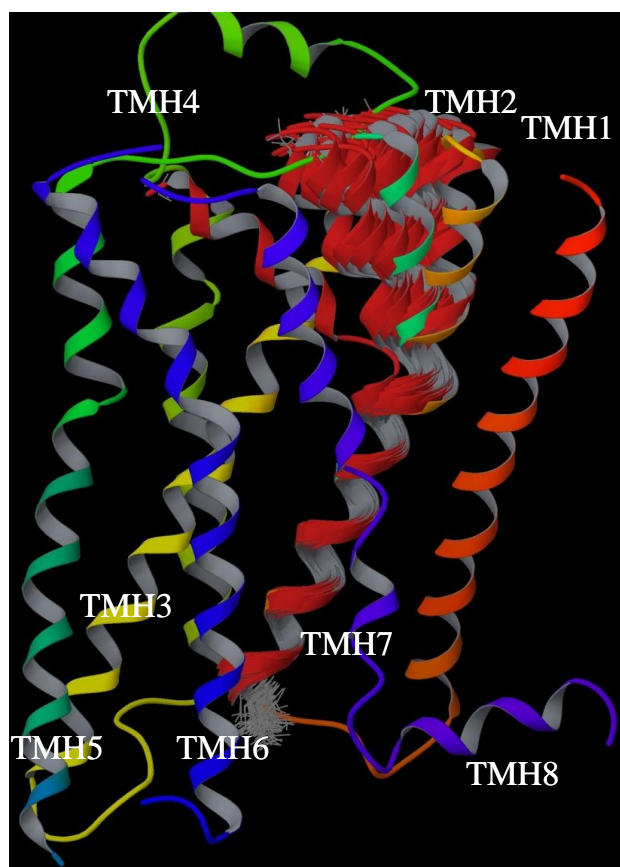


Figure 16. A side view of the 105 TMH2 helices from the CM runs superimposed on TMH2 of the  $\beta_2$ -adrenergic receptor is illustrated here. These helices were superimposed from the residue 2.38 to residue 2.53.

The strength of the CM method is based in allowing sampling of low free-energy conformations of a helix and to assess the ability of a helix-distorting residue (Pro, Gly or Ser) to affect the conformation of the helix. The limitation of this method is that the calculation is performed on an isolated helix, but the helix needed for the model is one that will be part of the TMH bundle and therefore must meet several steric constraints imposed by the receptor. Five helices from the CM runs met, in the context of a three dimensional model of the GPR55 receptor, the criteria used to identify a helix for bundle incorporation. The most important criterion used to select the appropriate helix required



that the EC-1 loop attachment be possible without overtightening of the helix ends (which would cause van der Waals overlap due to the short three residue EC-1 loop of GPR55 (SPF). The helix finally chosen for the bundle incorporation was helix number 40 from CM with a bend angle of  $36.8^\circ$ , a wobble angle of  $-81.5^\circ$ , and a face shift of  $62.0^\circ$ . When this helix was incorporated into the TMH bundle, the residues Ser 2.64 (residue 27), Leu 2.63 and Lys 2.60 were facing into the binding site crevice.

In helix 2 different GPCRs have a single proline at position 2.58, 2.59 or 2.60. Proline can be in different position and act as mimic of GGFT motif present in GPCRs. This results showed that shift by one position of the proline modified the angle between the pre-proline and post-proline helix.

### TMH5

CM calculations were used to explore the accessible conformations of GPR55 TMH5. TMH5 in GPR55 contains the highly conserved P5.50 that is used as an alignment guide for most class A GPCR's, but also contains a second proline at position P5.41. The average proline kink angle and standard deviation for each set of conformational results generated by CM were measured using the ProKink program (40). This program, which is part of Simulaid Conversion program was used to calculate the face shift, wobble angle, and bend angle of each helix. A statistical analysis of the resultant face shift, wobble angle and bend angle for the 105 helices containing the proline at position 5.41 (184) was performed using the statistical analysis package (GraphPad Software for one sample t test) and compared to TMH5 of the  $\beta_2$ -adrenergic

receptor which contains a proline at position 5.50. See Figure 17 for primary amino acid sequence of TMH5 in GPR55 vs. the  $\beta_2$ -adrenergic receptor.



Figure 17. Primary amino acid sequence of TMH5 in GPR55 and the  $\beta_2$ -adrenergic receptor.

As mentioned previously, the presence of proline residues in  $\alpha$ -helices can perturb the structure by introducing a distortion of this helical structure. This distortion is due to the avoided steric clash between the ring of the proline at position (i) and the backbone carbonyl at position (i-4), as well as the elimination of helix backbone H-bonds for the carbonyls at position (i-3) and (i-4).

Helix 5 was built based on the backbone of the Beta 2 adrenergic receptor and the region around P5.50 was restrained to preserve the initial structure as the Beta 2 adrenergic receptor. Only the flexible region containing P5.41 was varied because the effects of P5.41 on helix geometry are unknown and this can be solved using CM. The backbone torsions of residues K5.37 to P5.41 were varied  $\pm 50^\circ$

The region surrounding P5.50 in the  $\beta_2$ -adrenergic receptor is distorted, losing helicity in the local region rather than adopting a significant proline kink. This regional

distortion was incorporated into GPR55 TMH5 before CM calculations were performed. Table 3 lists the proline bend, wobble and face shift angles for the  $\beta_2$ -adrenergic receptor structure. GPR55 TMH5 has an additional proline residue at 5.41. The region around this proline was varied during CM calculations (see Methods). Table 4 lists the values for the bend, wobble and face shift angles for GPR55 TMH5 in the region of P5.41. It is clear here that P5.41 induces a different helix distortion compared to P5.50 in the  $\beta_2$ -adrenergic receptor. A comparison of the distortions is provided in Table 4 by using a one sample independent t test to analyze the means of the bend angle, wobble angle, and face shift for the GPR55 CM results containing P5.41 (184) compared to the crystal structure of  $\beta_2$ -adrenergic receptor (containing P 5.50). This test revealed that, at the  $p=0.05$  level, the difference of the population means of GPR55 CM results bend angle, wobble angle and face shift were significantly different from the TMH5 P5.50 region in the crystal structure of  $\beta_2$ -adrenergic receptor.

Table 4. Comparison of ProKink analysis of CM GPR55 TMH5 output vs Prokink analysis of TMH5 in the crystal structure of  $\beta_2$ -adrenergic receptor.

Proline Position	Bend Angle (degrees)	Face Shift (degrees)	Wobble Angle (degrees)
P 5.50 (211) ( $\beta_2$ -adrenergic)	6.0	79.0	-137.2
*P 5.41 (184) (GPR55)	**23.2 $\pm$ 7.3	**34.9 $\pm$ 16.5	-67.1 $\pm$ 138.9

\*Values are presented as mean  $\pm$  S.D.

\*\* Statistically significant difference at P 0.05 level in one-sample independent t test.

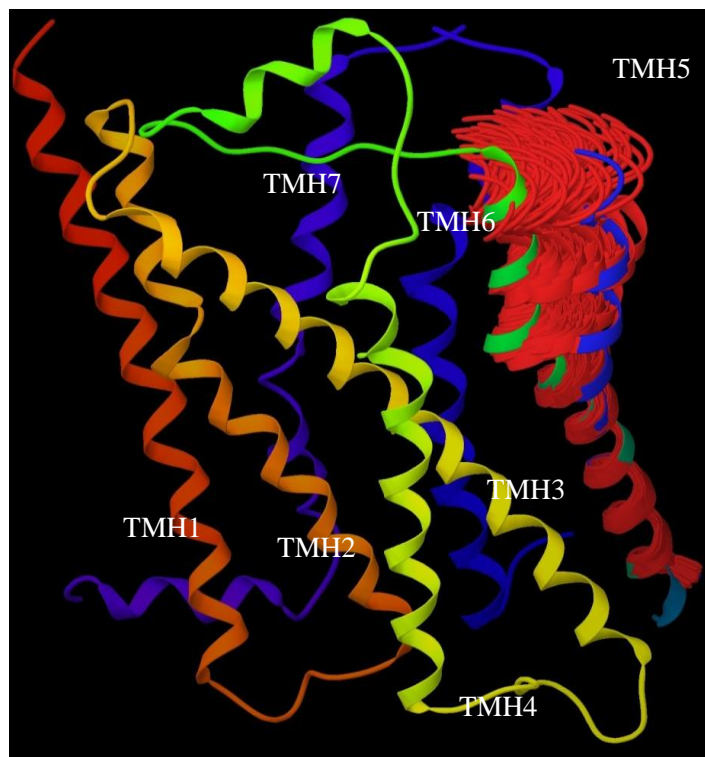


Figure 18. Illustrated here are side and extracellular views of the 105 TMH5 helices from the CM runs superimposed on TMH5 of the  $\beta_2$ -adrenergic receptor (from the residue 5.53 to residue 5.64).

Rho and  $\beta_2$ -adrenergic contain the conserved proline residue at position 5.50 compared to GPR55 which contains two proline residues. The conformational memories results showed a distortion of the helical structure to avoid steric clash between ring of proline and backbone carbonyl, contributing to the observed flexibility.

### TMH6

TMH6 is an important helix in the R to R\* transition, for this reason I studied the conformations accessible to TMH6 in GPR55 using CM. TMH6 in GPR55 does not have the class A GPCR highly conserved CWXP motif, but it contains the conservative

substitution in this motif: SFLP. See Figure 19 for the primary amino acid sequence of GPR55 TMH6 vs. that of the  $\beta_2$ -adrenergic receptor.

Helix 6 sequence	
	6 6
	4 5
	7 0
GPR55	QKACIYSIAASLAVFVVSFLPVHLGFFLQFLV
Beta-2	EHKALKTLGIIMGTFTLCWLPFFIVNIVHVIQ

Figure 19. Primary amino acid sequence of TMH6 in GPR55 and the  $\beta_2$ -adrenergic receptor.

The average proline kink angle and standard deviation for each set of conformational results generated by CM were measured using the ProKink program (40). This program, which is part of Simulaid Conversion program was used to calculate the face shift, wobble angle, and bend angle of each helix. A one sample independent t test was used to analyze the means of the bend angle, wobble angle, and face shift of the 105 helices containing proline at position 6.50 (GPR55 P6.50 (241)) and compared to the crystal structure of  $\beta_2$ -adrenergic receptor (  $\beta_2$ -adrenergic P6.50 (288)). This test revealed that, at the  $p=0.05$  level, the difference of the population means of the GPR55 CM results for wobble angle and face shift were significantly different from TMH6 in the crystal structure of  $\beta_2$ -adrenergic receptor, however, the bend angle was not significantly different (see Table 5).

Table 5. Comparison of ProKink analysis of Conformational Memories output vs Prokink analysis of TMH6 in the crystal structure of  $\beta_2$ -adrenergic receptor.

Proline Position	Bend Angle (degrees)	Face Shift (degrees)	Wobble Angle (degrees)
P 6.50 (288) ( $\beta_2$ -adrenergic)	33.2	84.9	-73.0
*P 6.50 (241) (GPR55)	$32.6 \pm 11.4$	$55.7 \pm 38.7$	$-90.1 \pm 74.2$

Values are presented as mean  $\pm$  S.D.

\*\* Statistically significant difference at P 0.05 level in one-sample independent t test.

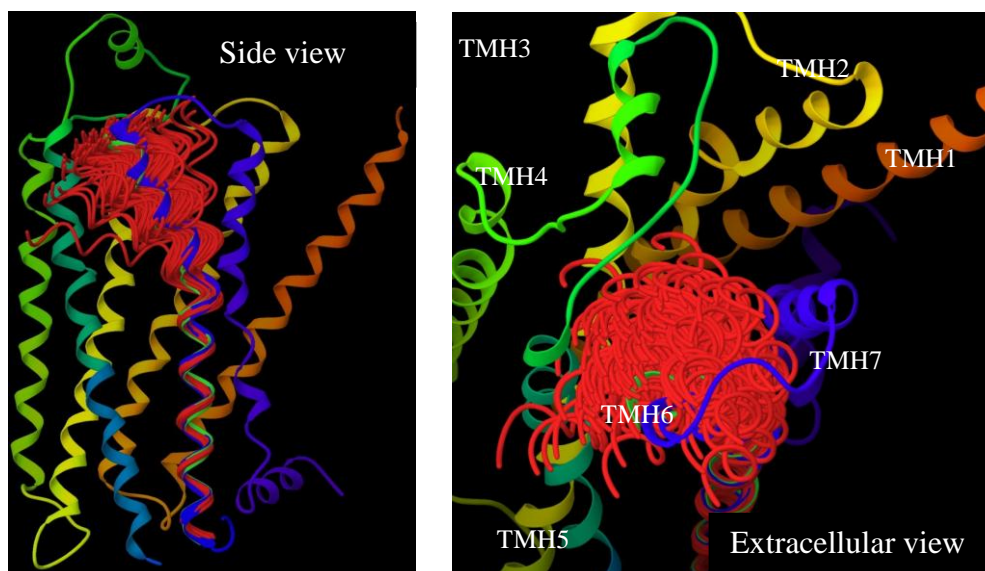


Figure 20. Illustrated here are side and extracellular views of the 105 TMH6 helices from CM runs for the GPR55 inactive state superimposed on TMH6 of the  $\beta_2$ -adrenergic receptor (from the residue 6.32 (223) to residue 6.45(236)).

In the  $\beta_2$ -adrenergic receptor, aromatic residues at 6.44 and 6.52 flank the toggle switch residue, W6.48. These residues, along with C6.47 have been proposed to be part

of a larger rotamer toggle switch within the binding site crevice of the  $\beta_2$ -adrenergic receptor (39). GPR55 also has aromatic residues flanking F6.48, F6.44 and H6.52, while the residue at 6.47 is a serine. To test the relation of the Serine 6.47 with the modulation of a possible GPR55 rotamer toggle switch (F6.44/F6.48/H6.52), the population of the  $\chi_1$  rotamer for each starting conformation based on the position of S6.47 was correlated with the position of the residues F6.48, F6.44 and H6.52 (see Table 6).

Table 6. The correlation of  $\chi_1$  of S6.47, F6.44, F6.48 and H6.52.

Ending rotamer		F 6.48			F 6.44			H 6.52		
		g-	g+	t	g-	g+	t	g-	g+	t
S 6.47	g+	0%	26%	74%	0%	15%	85%	0%	25%	75%
	t	0%	26%	74%	0%	10%	90%	0%	22%	78%
Javitch results		W 6.48			F 6.44			F 6.52		
		g-	g+	t	g-	g+	t	g-	g+	t
C 6.47	g+	---	39%	61%	----	----	----	----	23%	77%
	t	---	70%	30%	----	----	----	----	44%	56%

The results were compared to those reported by Javitch and Ballesteros in 2002 for  $\beta_2$ -adrenergic receptor ( $\beta_2$ -AR) (39). These results indicate that there is no correlation between the  $\chi_1$  of S6.47 and the  $\chi_1$  of the residues F6.44 (235), F6.48 (239) and H6.52 (243).

The next step was to test if there is a correlation between the  $\chi_1$  of F6.48 and the  $\chi_1$ 's of F6.44(235) and H6.52(243). The results of this study are summarized in Table 7.

Table 7. The correlation of  $\chi_1$  of F6.48 (239) with F6.44 (235) and H6.52 (243)

<b><math>\chi_1</math> of serine 6.47 (238) was held in trans position</b>							
		F 6.44		H 6.52			
		g plus	trans	g plus	trans	Bend angle	Wobble angle
F 6.48	g plus	30.%	70.%	81.%	19.%	*40.5 $\pm$ 16.3	*-56.7 $\pm$ 60.5
	trans	4.%	96.%	3.%	97.%	*29.9 $\pm$ 7.6	*-101.7 $\pm$ 74.7

\*Values are presented as mean  $\pm$  SD.

The results indicate that there is a correlation between the  $\chi_1$  of F6.48 (239) and  $\chi_1$  of H6.52. When the  $\chi_1$  of F6.48 (239) is in g-plus (inactive state conformation), the  $\chi_1$  of H6.52 prefers the g plus position. When the  $\chi_1$  of F6.48 (239) is in trans position (activated state), the  $\chi_1$  of H6.52 prefers the trans position. Results for F6.44, suggest that trans position is favored for F6.44 whether the  $\chi_1$  of F 6.48(239) is g-plus or trans. There is, however, a lessening of the number of helices with  $\chi_1$  of F6.44 in trans when the  $\chi_1$  of F6.48 is g-plus (96%  $\rightarrow$  70%), but a trans  $\chi_1$  for F6.44 is clearly still favored.

Results in Table 7 also show that although there is a trend in the bend angle of TMH6 towards less bent helices when F6.48 undergoes a  $\chi_1$  g $\rightarrow$  trans change, this is not statistically significant. This result is not consistent with experimental evidence that TMH6 straightens during activation.

### TMH7

Figure 21 illustrates the sequence alignment for GPR55 TMH7 vs. that of the  $\beta_2$ -adrenergic receptor. TMH7 in Class A GPCRs usually has the conserved sequence motif, NPXXY, which not only influences the conformation of TMH7, but also places Y7.53 in the correct position to interact with F7.60 on the intracellular extension of TMH7, Hx8.



The preferred conformation of TMH7 in GPR55 was studied because it lacks the NPXXY motif in TMH7. Instead, this region of the sequence is DVFCY in GPR55. C7.46 to V7.50 was considered the flexible region in CM calculations. The output of the CM was superimposed on the  $\beta_2$ -adrenergic receptor ( $\beta_2$ -AR) template from residue F7.51 (286) to V7.56 (291) (intracellular region) (Figure 21).

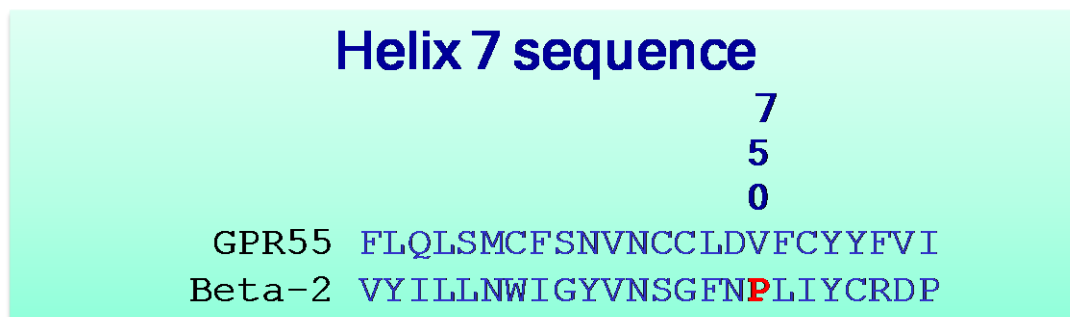


Figure 21. Primary amino acid sequence of TMH7 in GPR55 and the  $\beta_2$ -adrenergic receptor.

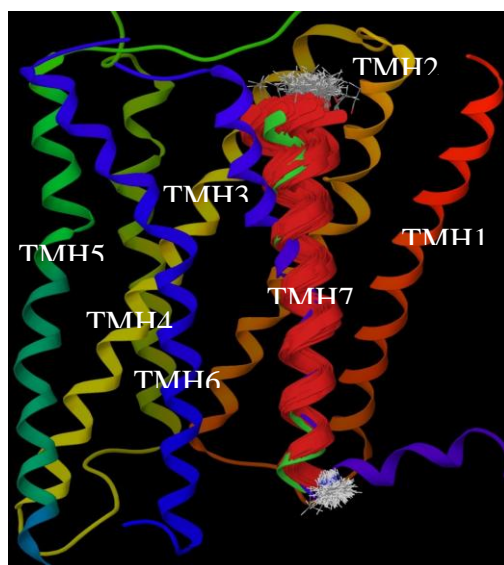


Figure 22. Side view of the TMH7 CM output helices superimposed to the ( $\beta_2$ -adrenergic receptor.

Table 8. Comparison of ProKink analysis of CM output vs Prokink analysis of TMH7 in the crystal structure of  $\beta_2$ -adrenergic receptor

Proline Position	Bend Angle (degrees)	Face Shift (degrees)	Wobble Angle (degrees)
P 7.50 ( $\beta_2$ -adrenergic)	20.1	9.1	161.4
*V 7.50 (GPR55)	**10.1 $\pm$ 4.7	16.9 $\pm$ 144.2	**16.8 $\pm$ 11.6

\*Values are presented as mean  $\pm$  S.D.

\*\* Statistically significant difference at P 0.05 level in one-sample independent t test.

$\beta_2$  adrenergic receptor contains a proline in position P7.50 which forms part of the motif NPXXY but GPR55 lacks the proline residue in position P7.50. The output of

the conformational memories showed a decreased bend compared to the  $\beta$ -2 adrenergic receptor.

#### Helix 8 GPR55

The intracellular extension of TMH7, Hx8 ((E 7.59 (294) – A 7.86 (319)) was modeled in the same conformation seen in the Rho structure and the receptor was truncated after A7.86.

#### Model of Inactive state (R) and active state form of GPR55

A model of the R and R\* form of GPR55 was created using the crystal structure of the  $\beta_2$ -adrenergic receptor as a starting point. The sequence of the human GPR55 receptor (see Figure 24) was aligned with the sequence of the  $\beta_2$ -adrenergic receptor using highly conserved residues across Class A GPCRs as alignment guides. Results from CM were used to substitute TMH2, TMH5, TMH6 and TMH7 for existing helices in GPR55 model. Loops affected by the replacement of TMH2 (IC-1, EC-1), TMH5 (EC-2, IC-3), TMH6 (IC-3, EC-3), TMH7 (EC-3) were modeled using Modeller program. OPLS\_2005 all atom force field in Macromodel 9.1 was used to energy minimize the GPR55 R and R\* models.

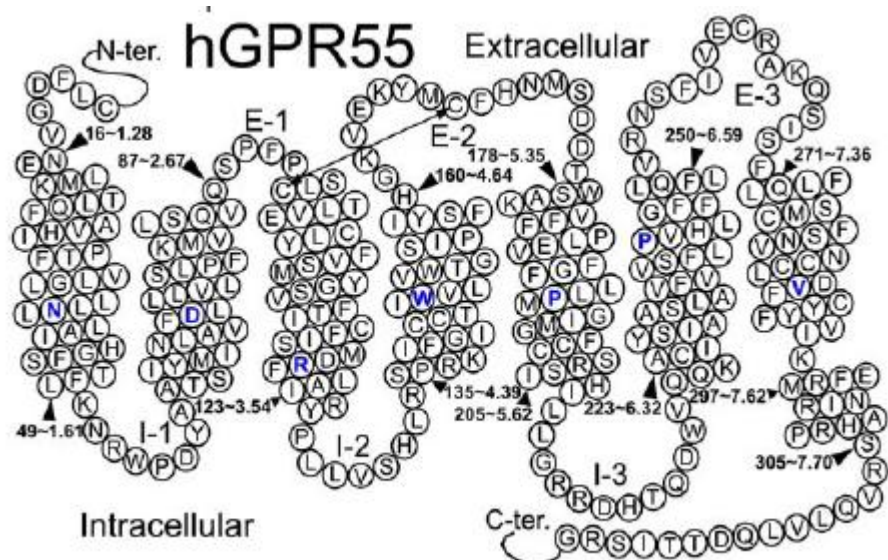


Figure 23. Schematic representation of human GPR55 receptor. The most highly conserved residue in each helix is highlighted in blue.

The biophysical studies reporting the changes that occur during the R to R\* transition from Rho and the  $\beta_2$ -adrenergic receptor are the bases for the creation of the GPR55 model active state (R\*) (19). These studies indicated the rotation of TMH3 and TMH6 and a conformational change in TMH6 (straightening in the CWXP hinge region of TMH6) which occurs upon activation. An R\* GPR55 model was created including a TMH6 conformer derived from our conformational memories study of GPR55 TMH6.

## CHAPTER V

### DISCUSSION

In the present study, I used the Conformational Memories (CM) technique to explore the sequence dictated conformation of key helices: TMH2, TMH5, TMH6 and TMH7 in GPR55 and compared these results to the  $\beta_2$ -adrenergic receptor structure (44).

#### TMH2

Many GPCR's contain Pro at position 2.59 or 2.58 so the bend is present at the residues 2.55 to 2.59 or 2.58 in the helix turn formed by the Pro-kink at the similar positions as the bend in rhodopsin, which contains the motif Gly-Gly-X-Thr-Thr instead of proline.

Different GPCR's have a single Pro at position 2.58, 2.59 or 2.60 and each one of these positions would be expected to orient the bend differently. The fact that the Pro can be in different positions and act as mimic of the motif Gly-Gly-X-Thr-Thr suggest that this may be a source of considerable structural diversity in the Class A receptors.

Our CM analysis of TMH2 in GPR55 compared to the TMH2 of the  $\beta_2$ -adrenergic receptor showed that the shift by one position of the amino acid proline (GPR55 containing P2.58 (78) compared to the crystal structure of  $\beta_2$ -adrenergic receptor containing P2.59) produces a significant difference in the bend angle and face shift of TMH2.

Meaning that the different position of proline modified the angle between the two parts (pre-proline and post-proline) of the TMH2 in GPR55 compared to the  $\beta_2$ -adrenergic receptor, causing a shift of the amino acids as a result of the presence of the proline bend. The presence of the serine residue in position 2.56(76), satisfied its hydrogen-bonding capacity by an intrahelical hydrogen bond interaction between the O- $\gamma$  atom and the i-4 carbonyl oxygen of the residue Leu 2.52(72) stabilizing the bend angle created by the presence of the proline.

### TMH5

In Rho and the  $\beta_2$ -adrenergic receptor there is a single proline residue in TMH5 at position 5.50, which causes a deviation from normal alpha-helicity in the region, 5.46-5.50. TMH5 in GPR55 has two proline residues (P5.40 and P5.50). The CM results showed a difference of the population means of GPR55 in the bend angle, wobble angle and face shift (for P5.40) compared to the TMH5 in the crystal structure of  $\beta_2$ -adrenergic receptor (for P5.50). The distortion of the helical structure results from the avoidance of a steric clash between the ring of the proline at position (*i*) and the backbone carbonyl at position (*i* – 4), as well as the elimination of helix backbone hydrogen bonds for the carbonyls at positions (*i* – 3) and (*i* – 4). These two factors (departure from the ideal helical pattern and the reduction in hydrogen-bond stabilization) contribute to the observed flexibility of a proline-containing –helix, which is illustrated in Figure 24.

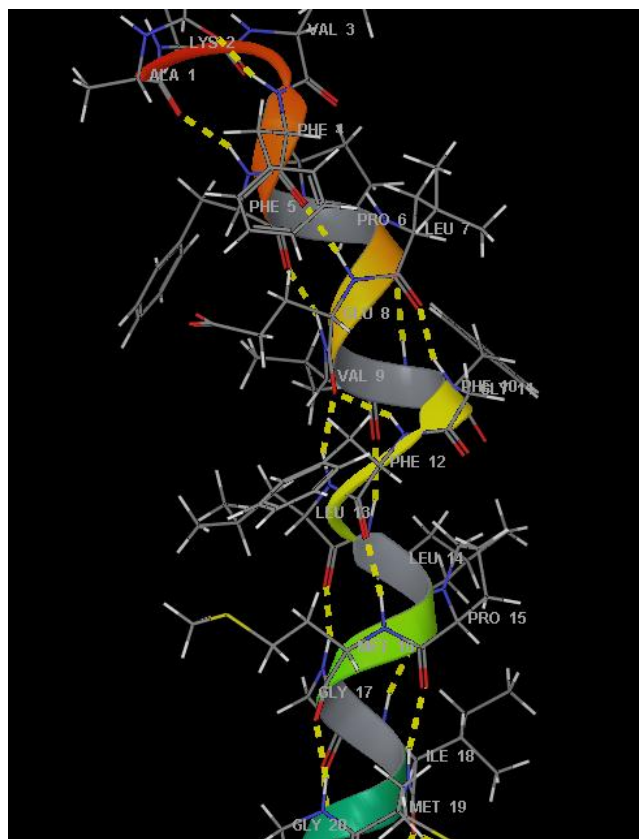


Figure 24. Presence of proline causes a distortion of the helical structure. This figure shows how the presence of proline at position 5.50 causes the helical portion to be disrupted between the leucine 5.48 (#13 in figure) and phenylalanine 5.47 (#12 in figure).

### TMH6

TMH6 in GPR55 does not have the Class A GPCR highly conserved CWXP motif. However, it has the conservative substitutions of this motif: SFLP. Since TMH6 has been implicated in conformational changes during receptor activation, it was important to study the allowed conformations of TMH6. It has been reported during the activation process of the GPCRs, that agonist binding influences the rotameric state of aromatic residues in TM6 altering the configuration of TMH6 prokink which in turn results in movement of the cytoplasmic end of TMH6 away from TMH3. For the  $\beta_2$ .

adrenergic receptor, the residue C6.47 has been reported to modulate the configuration of aromatic cluster surrounding the proline kink and the proline kink itself (45). The cluster of highly conserved aromatic residues surrounding the proline kink includes Phe 6.44, Trp 6.48 and Phe 6.52 in the  $\beta_2$ –adrenergic receptor, all of which face into the binding site crevice. In the case of GPR55, the residues forming the aromatic cluster are F6.48, F 6.44 and H 6.52. To test the ability of Serine 6.47 to modulate the aromatic cluster (as suggested by the results of Shi and co-workers for the  $\beta_2$ –adrenergic receptor (Shi et al., 2002)), the population of the  $\chi_1$  rotamers for each starting conformation based upon the rotameric state of S 6.47 was correlated with the position of the residues F 6.48, F 6.44 and H 6.52 (see Table 5). These results did not show a correlation between the position of the rotameric state of S6.47 and the  $\chi_1$  position of the residues F6.44, F 6.48 and H 6.52. However, there was a correlation between the rotameric state of residue H6.52 based on the position of F 6.48 (See results in Table 6). When the  $\chi_1$  of F6.48 (239) is in g-plus (inactive state conformation), the  $\chi_1$  of H6.52 prefers the g plus position. When the  $\chi_1$  of F6.48 (239) is in trans position (activated state), the  $\chi_1$  of H6.52 prefers the trans position. In contrast, results for F6.44, suggest that trans position is favored for F6.44 whether the  $\chi_1$  of F 6.48(239) is g-plus or trans. The resulting simulation structure can be clustered into two major groups based in the rotamer conformation of 6.48 and 6.52: (1) F 6.48 g plus/ H 6.52 g plus and (2) F 6.48 trans/H 6.52 trans.

Although the results in Table 6 suggest a trend in the F 6.48  $\chi_1$  g+  $\rightarrow$  trans change towards less bent helices, this trend is not statistically significant. This result, therefore, is not consistent with biophysical studies that show that during activation



P6.50, in the region CWXP region of TMH6 can act as a flexible hinge allowing TMH6 to straighten upon activation. This movement would result in its intracellular end moving away from TMH3 and upwards towards the lipid bilayer.

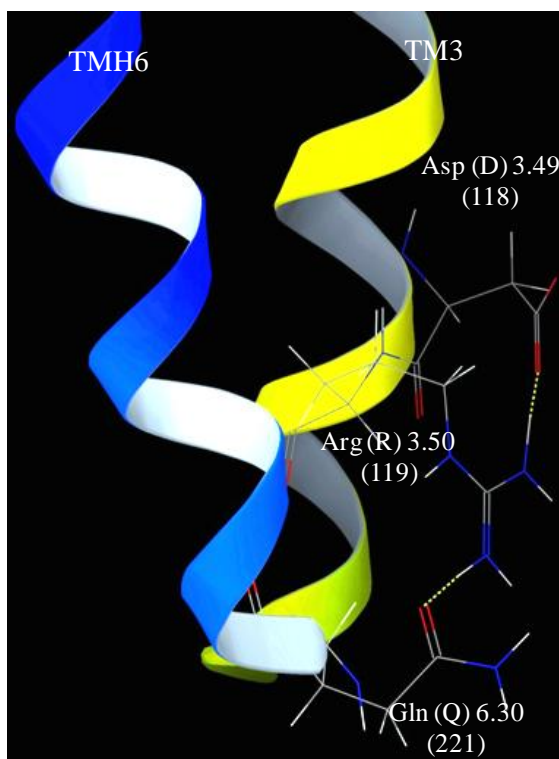


Figure 25. Ionic lock in GPR55 inactive state

There is evidence that activation is accompanied by rigid domain motion of TMH3 and TMH6. In the intracellular ends of TMH3 and TMH6 there is a constrained by D3.49 (118); R3.50 (119) and Q6.30 (221) forming a salt bridge that limits the mobility of the cytoplasmic ends and acts like ionic lock. During activation, P6.50 acts as

a flexible hinge, permitting TMH6 to straighten upon activation and move its intracellular end away from TMH3 and up toward the lipid bilayer

The residue F6.48 has been reported to change conformation upon activation:

R  $\chi_1$  g $\rightarrow$ trans in R\*

Many GPCRs have aromatic residues that flank W6.48, acting as a toggle switch with possible correlated movements of flanking aromatic residues such as F6.44 and H6.52 in GPR55 as shown in figure 26.

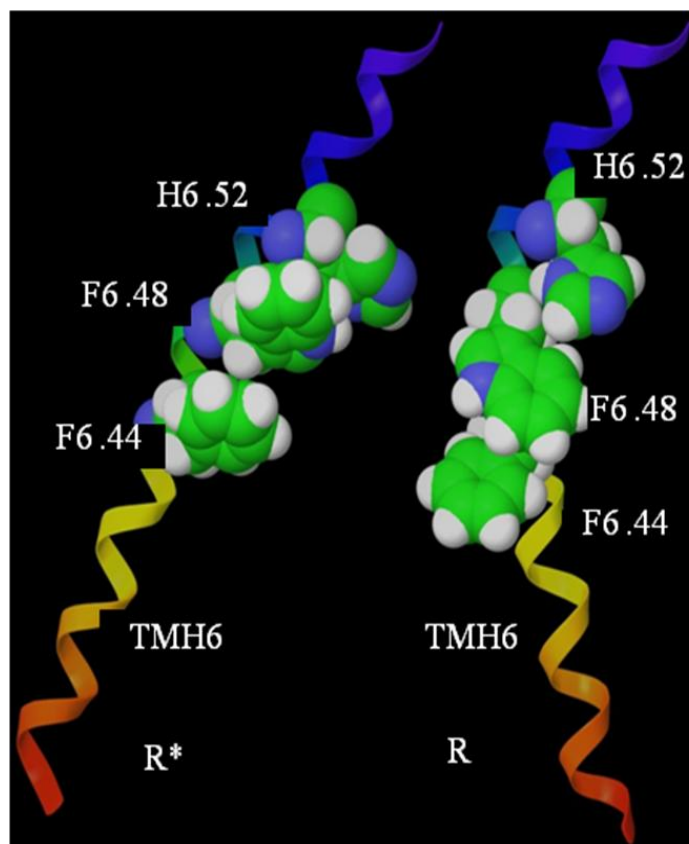


Figure 26. Toggle switch in GPR55.

The correlation of  $\chi_1$  of F6.48 (239) with F6.44(235) and H6.52 (243) are reported in table 9.

Table 9. Correlation of  $\chi_1$  of F6.48 (239) with F6.44(235) and H6.52 (243).

<b><math>\chi_1</math> of serine 6.47 (238) was held in trans position</b>							
		F 6.44		H 6.52			
		g plus	trans	g plus	trans	Bend angle	Wobble angle
<b>F 6.48</b>	<b>g plus</b>	30%	70%	81%	19%	*40.53 ± 16.26	*-56.73 ± 60.50
	<b>trans</b>	4%	96%	3%	97%	*29.91 ± 7.64	*-101.65 ± 74.67

Values are presented as mean ± SD

The results shown:

- F6.44 prefers trans: Population does not correlate with F6.48  $\chi_1$
- H6.52  $\chi_1$  correlates with F6.48  $\chi_1$
- When F6.48  $\chi_1$  is g+, H6.52  $\chi_1$  prefers g+
- When F6.48  $\chi_1$  is trans, H6.52  $\chi_1$  prefers trans

The main point used to assemble the model of active and inactive GPR55 receptor were:

- No Van der Waals overlaps with other TMHs in the bundle
- The extracellular end of TMH2 must be close enough to the extracellular end of TMH3
- The GPR55 EC-1 loop (SPF) contains half of the number of residues as Rho (GYFVFG).

- The attachment of EC-1 loop must be possible without over tightening the TMH backbone that would cause Van der Waals overlaps.
- Based on biophysical literature on the R to R\* transition in Class A GPCRs,
- Activation is accompanied by a straightening of TMH 6
- Activated model of GPR55
- conformer chosen for R\* bundle in which the proline kink angle is moderated in TMH 6
- F6.48  $\chi_1$  is in trans and H6.52  $\chi_1$  is in trans

Following these points we obtained the models shown in figure 27.

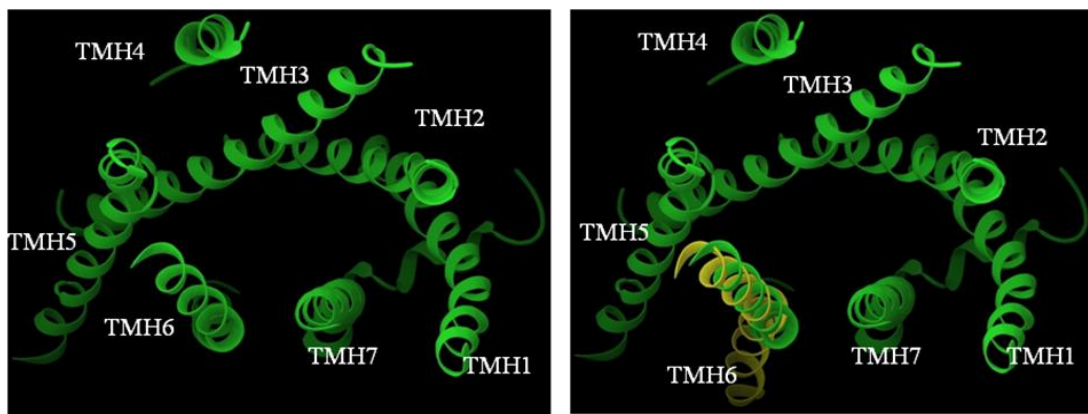


Figure 27 Inactive receptor GPR55 top view ( left figure) and active receptor GPR55 (right figure).

### TMH7

The preferred conformation of TMH7 in GPR55 was studied because it lacks the NPXXY motif in TMH7. Instead, this region of the sequence is DVFCY in GPR55. The

output of the CM showed that without the presence of proline, the helix is less bent compared to the beta adrenergic receptor TMH7.

## CHAPTER VI

### CONCLUSIONS

In conclusion, the results of the CM analysis of GPR55 are consistent with the proposal of Ballesteros et al.(46) , that even though the overall structure of Rho and other class A GPCRs may be very similar, there are localized regions where the structure of these receptors diverges. A significant range of conformational diversity could be generated within the binding site crevice of different GPCRs by the presence of Pro-kinks and Cys/Ser/Thr residues. The presence of different amino acids or alternate microdomains may support very similar deviations from regular  $\alpha$ -helical structure, resulting in a similar tertiary structure. This could be a mechanism by which the different receptors could diverge sufficiently to develop the selectivity necessary to interact with diverse ligands, while still maintaining a similar overall fold in the core function. The core function is the signaling activation through a conformational change in the TMHs that alters the conformation of the cytoplasmic surface and subsequent interaction with G-proteins. This core function is shared by the entire Class A GPCR family of receptors, despite their selectivity for a diverse group of ligands. In this thesis, the consequence of sequence divergences in GPR55 was explored. The results reported here should help to define the mechanism of drug-receptor interaction relevant to cannabinoid physiological and pathophysiological functions including drug abuse.

## REFERENCES

1. Behavioral effects of cannabinoid agents in animals By Chaperon F, Thiebot MH  
INSERM U.288 and Department of Pharmacology, Faculty of Medicine Pitie-Salpetriere,  
Paris, France. Crit Rev Neurobiol 1999; 13(3):243-81
2. Brown, A., S. Ueno, K. Suen, S. Dowell, and A. Wise. Molecular identification of  
GPR55 as third G-protein coupled receptor responsive to cannabinoid ligands. In 2005  
symposium of the cannabinoids. 2005. Clear water, Fl: International Cannabinoid  
Research Society.
3. Sjogren, S., E. Ryberg, A. Lindblom, N. Larsson, A. Astrand, S.Hjorth, A. Anderson,  
T.Groblewski and P. Greasley. A new receptor for cannabinoid ligands. In 2005  
symposium on the cannabinoids. 2005. Clearwater, FA: International Cannabinoid  
Research Society.
4. O'Dowd, B.F., T.Nguyen, A. Marchese, R. Cheng, K.R. Lynch, H.H. Heng, L.F.  
Kolaskowski, Jr., and S.R. George, Discovery of three novel G-protein-coupled receptor  
genes. Genomics, 1998. 47(2):p. 310-3.
5. Di Marzo, V., C.S. Breivogel, Q. Tao, D.T. Bridgen, R.K. Razdan, A.M. Zimmer, A.  
Zimmer, and B.R. Martin, Levels, metabolism, and pharmacological activity of  
anandamine in CB1 cannabinoid receptor knockout mice: evidence for non-CB1, non-  
CB2 receptor-mediated actions of anandamine in mouse brain. J Neurochem, 2000.  
75(6): p. 2434-44.
6. Brown, A. and A.Wise, Identification of modulators of GPR55 activity. WO0186305.  
2003. GlaxoSmithKline: USPTO.
7. Drmota, T., P. Greasley, and T. Groblewski, Screening assays for cannabinoids-ligand  
type modulators of GPR55. 2004, Astrazeneca: USA.
8. Skaper, S.D., A. Buriani, R.D. Toso, L. Petrelli, S. Romanello, L. Facci, and A. Leon,  
The ALIAmide palmitoylethanolamide and cannabinoids, but not anandamine, are  
protective in delayed postglutamate paradigm of excitotoxic death in cerebellar granule  
neurons. Proc. Natl. Acad. Sci. USA. 1996. 93 (April): p. 3984-3989.

9. Jaggar, S., S. Sellaturay, and A. Rice, The endogenous cannabinoid anandamine, but not the CB2 ligand palmitoylethanolamide, prevents the viscerovisceral hyper-reflexia associated with inflammation of the rat urinary bladder. *Neurosci. Lett.*, 1998. 253 (2): p. 123-126.
10. Sawzdargo, M., T. Nguyen, D.K. Lee, K.R. Lynch, R. Cheng, H.H. Heng, S.R. George, and B.F. O'Dowd, Identification and cloning of three novel human G protein-coupled receptor genes GPR52, GPR53 and GPR55: GPR55 is extensively expressed in human brain. *Brain Res Mol Brain Res*, 1999. 64(2): p. 193-8.
11. Friderie, E., D. Ponde, A. Breuer, and L. Hanus, Peripheral, but not central effects of cannabinoid derivatives; Mediation by CB1 and unidentified receptors. *Neuropharmacology*, 2005. 48(8): p. 1117-29. Epub 2005 Apr 2006.
12. Pertwee RG. GPR55: a new member of the cannabinoid receptor clan? *Br J Pharmacol*. 2007 Dec; 152(7): p. 984-6.
13. Staton PC, Hatcher JP, Walker DJ, Morrison AD, et al. The putative cannabinoid receptor GPR55 plays a role in mechanical hyperalgesia associated with inflammatory and neuropathic pain. *Pain*. 2008 May 23: p. 1-12.
14. Waldeck-Weiermair M, Zoratti C, Osibow K, Balenga N, Goessnitzer E, et al. Integrin clustering enables anandamide-induced  $Ca^{2+}$  signaling in endothelial cells via GPR55 by protection against CB1-receptor-triggered repression. *J Cell Sci*. 2008 May 15; 121: p. 1704-17
15. Lauckner JE, Jensen JB, Chen HY, Lu HC, Hille B, Mackie K. GPR55 is a cannabinoid receptor that increases intracellular calcium and inhibits  $M$  current. *Proc Natl Acad Sci U S A*. 2008 Feb 19. ; 105(7):2699-704.
16. Oka S, Nakajima K, Yamashita A, Kishimoto S, Sugiura T. Identification of GPR55 as a lysophosphatidylinositol receptor. *Biochem Biophys Res Commun*. 2007 Nov 3;362(4) :928-34.
17. Palczewski, K., T. Kumasaka, T. Hori, C.A. Behnke, H. Motoshima, B.A. Fox, I. Le Trong, D.C. Teller, T. Okada, R.E. Stenkamp, M. Yamamoto, and M. Miyano. Crystal structure of rhodopsin: A G protein-coupled receptor. *Science*, 2000. 289 (5480): p. 739-45.
18. Okada, T., Y. Fujiyoshi, M. Silow, J. Navarro, E.M. Lauda, and Y. Shichida, Functional role of internal water molecules in rhodopsin revealed by X-ray crystallography. *Proc Natl Acad Sci USA*, 2002. 99(9): p5982-7.



19. Li, J., P. C. Edwards, M. Burghammer, C. Villa, and G.F. Schertler, Structure of bovine rhodopsin in a trigonal crystal form. *J Mol Biol*, 2004. 343(5): p. 1409-38.
20. Picone, R. P., A. D. Khanolkar, W. Xu, L.A. Ayotte, G.A. Thakur, D.P. Hurst, M.E. Abood, P.H. Reggio, D.J. Fournier, and A. Makriyannis, (-)-7'-Isothiocyanato -11-hydroxy-1',1'-diethylheptylhexahydrocannabinol (AM841), a high-affinity electrophilic ligand, interacts covalently with a cysteine in helix six and activates the CB1 cannabinoid receptor. *Mol Pharmacol*, 2005.68(6): p.1623-35.
21. Kapur A, Hurst D.P, Fleischer D, Whitnell R, Thakur G, Makriyannis A, Reggio P.H., Abood M.E. Mutations studies of Ser 7.39 and Ser 2.60 in the human CB1 cannabinoid receptor: evidence for Serine-Induced Bend in CB1 transmembrane helix 7. *Molecular pharmacology* 2007. Vol.71 N0.6 p 1512-1524.
22. McAllister S.D., Rizzi G., Anayi-Goffer S., Hurst D.P. Barnett-Norris J., Lynch D.L, Reggio P.H., Abood M.E. An aromatic microdomain at the cannabinoid CB1 receptor constitutes an agonist/inverse agonist binding region. *J. Med.Chem.* 2003. vol 46, p 5139-5152.
23. Hurst D., Umejiego U., Lynch D., Seltzman H., Hyat S., Roche M., McAllister S., Fleischer D., Kapur A., Abood M., Shi Shanping, Jones J., Lewis D., Reggio P. Biarylpyrazole inverse agonist at the cannabinoid CB1 receptor: important of the C-3 carboxamide oxygen/lysine3.28 (192) interaction. *J. Med. Chem.*, 2006, 49 (20) p 5969-5987.
24. Farrens, D., C. Altenbach, K. Ynag, W. Hubbel, and H. Khorana, Requirement of rigid-body motion of transmembrane helices for light activation of rhodopsin. *Science*, 1996. 274: p.768-70.
25. Ghanouni, P., J.J. Steenhuis, D.L. Farrens, and B.K. Kobilka, Agonist-induced conformational changes in the G-protein-coupling domain of the beta 2 adrenergic receptor. *Proc Natl Acad Sci U S A*, 2001. 98(11): p. 5997-6002.
26. Lin S.W. and T.P. Sakmar, Specific tryptophan UV-absorbance changes are probes of the transition of rhodopsin to its active state. *Biochemistry*, 1996.35(34): p.1149-59.
27. Javitch, J.A., D. Fu, G. Liapakis, and J. Chen, Constitutive activation of the beta 2 adrenergic receptor alters the orientation of its sixth membrane-spanning segments. *J Biol Chem*, 1997. 272(30): p. 18546-9.
28. Jensen, A.D., F. Guarnieri, S.G. Rasmussen, F. Asmar, J.A. Ballesteros, and U. Gether, Agonist-induced conformational changes at the cytoplasmic side of

transmembrane segments 6 in the beta 2 adrenergic receptor mapped by site selective fluorescent labeling. *J Biol Chem*, 2001. 276(12): p.9279-90.

29. Nakanishi, J., T. Takarada, S. Yunoki, Y. Kikuchi, and M. Maeda, FRET-based monitoring of conformational change of the beta2 adrenergic receptor in living cells. *Biochem Biophys Res Commun*, 2006. 343(4): p.1191-6.

30. Zhang Rundong, Hurst Dow, Barnett-Norris Jusy, Reggio Patricia and Song Zhao-Hui, Cysteine 2.59(89) in the second transmembrane domain of human CB2 receptor is accessible within the ligand binding crevice: Evidence for possible CB2 deviation from a Rhodopsin template. *Mol Pharmacol*, 2005.68(1): p.69-83.

31. Borhan, B., Souto M.L., Imai H., Shichida Y., Nakanishi K. Movement of retinal along the visual transduction path. *Science*, 2000. 288 (5474) : p. 2209-12.

32. Shi L, Liapakis G, Xu R, Guarnieri F, Ballesteros JA, and Javitch J A.  $\beta$ -2 adrenergic receptor activation. Modulation of the proline kink in transmembrane 6 by a rotamer toggle switch. *J Biol Chem* 2002. 277: 40989-40996.

33. Singh, R., Hurst D.P., Barnett –Norris J., Lynch D.L., Reggio P.H., Guarnieri F. Activation of the cannabinoid CB1 receptor may involve a W6.48/F3.36 rotamer toggle switch. *J Pept Res*, 2002. 60 (6):p. 357-70.

34. McAlister S.D., Hurst D.P., Barnett-Norris J., Lynch D., Reggio P.H., Abood M.E., Structural mimicry in class A G protein-coupled receptor rotamer toggle switches: the importance of the F3.36 (201)/W6.48(357) interaction in cannabinoid CB1 receptor activation. *J Biol Chem*, 2004. 279(46): p. 48024-37.

35. Barnett-Norris J., Hurst D.P., Buehner K., Ballesteros J.A., Guarnieri F., Reggio P.H., Agonist alkyl tail interaction with cannabinoid CB1 receptor V6.43/I6.46 groove induces a helix 6 active conformation. *Int. J. Quantum Chem.*, 2002. 88(1): p.76-86.

36. Ballesteros J. A. and H. Weinstein, Integrated methods for the construction of three dimensional models and computational probing of structure function relations in G-protein coupled receptor., in *Methods in Neuroscience*, S.C. Sealfon, Editor. 1995, Academic Press: San Diego, CA. p. 366-428 – Chapter 19.

37. Sawzdargo, M., T Nguyen, D.K. Lee, K.R. Lynch, R. Cheng, H.H. Heng, S.R. George, and B.F. O'Dowd, Identification and cloning of three novel human G protein-coupled receptor genes GPR52, GPR53 and GPR55: GPR55 is extensively expressed in human brain. *Brain Res Mol Brain Res*, 1999. 64(2):p.193-8.

- 38 Prioleau, C., I. Visiers, B.J. Ebersole, H. Weinstein, and S.C. Sealton, Conserved helix 7 tyrosine acts as a multistate conformational switch in the 5HT<sub>2C</sub> receptor. Identification of a novel “locked on” phenotype and double revertant mutations. *J Biol Chem*, 2002. 277(39): p. 36577-84 Epub 2002 Jul 26.
39. Fritze, O., S. Filipek, V. Kuksa, K. Palczewski, K.p. Hoffmann, and O.P. Ernst, Role of the conserved NPxxY(x)5,6F motif in the rhodopsin ground state and during activation. *Proc Natl Acad Sci U S A*, 2003. 100(5): p. 2290-5
40. Visiers Irache, Mraunheim Benjamin, Weinstein Harel. Prokink: a protocol for numerical evaluation of helix distortion by proline. *Protein Engineering*, 2000. 13(9): p.603-606.
41. Whitnell R. M., Hurst D. P, Reggio P. H., Guarnieri F.. “Conformational Memories with Variable Bond Angles”, *J. Comput. Chem.* in press (2007).
42. Fiser, A., R.K. Do, et al. Modeling of loops in protein structures. *Protein Sci* 2000. 9 (9):p 1753-73.
43. Sali ,A and T.L. Blundell. Comparative protein modeling by satisfaction of spatial restraints. *J Mol Biol* 1993. 234 (3): p. 779-815.
44. Cherezov V, Rosenbaum DM, Hanson MA, Rasmussen SG, Thian FS, Kobilka TS, Choi HJ, Kuhn P, Weis WI, Kobilka BK and Stevens RC (2007) High-resolution crystal structure of an engineered human beta2-adrenergic G protein-coupled receptor. *Science* 318(5854):1258-1265.
45. Shi L, Liapakis G, Xu R, Guarnieri F, Ballesteros JA and Javitch JA (2002) Beta 2 adrenergic receptor activation. Modulation of the proline kink in transmembrane 6 by a rotamer toggle switch. *J Biol Chem* 277(43):40989-40996
46. Ballesteros JA, Shi L, and Javitch JA. Structural mimicry in G-protein-coupled receptors: implication of the high-resolution structure of rhodopsin for structure-function analysis of rhodopsin like receptors. *Mol Pharmacol* 2001 (60): 1-19